Polysaccharide beads and films for controlled release of agricultural compounds and water decontamination

by

Mei Li

A dissertation submitted to the Graduate Faculty of
Auburn University
in partial fulfillment of the
requirements for the Degree of
Doctor of Philosophy

Auburn, Alabama
Dec 10, 2016

Keywords: polysaccharide, bead, film, sorption, controlled release

Approved by

Gisela Buschle-Diller, Chair, Professor of Biosystems Engineering
Maria Auad, Associate Professor of Chemical Engineering
Xinyu Zhang, Associate Professor of Chemical Engineering
Thomas Elder, Professor, USDA Forest Service

Abstract

Massive amounts of agricultural, industrial, medical and domestic water worldwide are polluted by different types of contaminants that harm the environment and impact human health. Films and beads made from abundant inexpensive polysaccharides have been shown to be effective sorbents that can be utilized for the removal of contaminants from effluent. In addition, these materials can also function as vehicles for controlled release of chemicals for targeted applications. As a result, polysaccharides properties have been exploited in various fields of research in the biomedical, pharmaceutical, cosmetic, food and agricultural industries due to their unique physicochemical characteristics.

In the first part of this research, alginate beads were formed by combination with either starch, one of two types of cellulose, or xylan as fillers and investigated for their effectiveness as sorbents in waste water remediation processes. Their capacity for water uptake, their sorption capabilities for a model cationic pollutant and their charge density was studied in relationship to their composition and their surface characteristics. The effect of drying the beads in air or lyophilizing on their average diameters was assessed by optical microscopy and differences in morphology were observed by scanning electron microscopy. Their interaction with water was evaluated using low-field NMR spectroscopy. It was found that nanocrystalline cellulose had the most influence on the beads' sorption capacity for cationic contaminants while xylan admixture created beads with the highest water sorption after lyophilization.

In the second part of this research, polysaccharide beads formulated from alginate, cellulose powder, cellulose nanocrystals (CNC), starch and xylan were reinforced with kaolin and surface-modified with polyethylenimine (PEI), a positively-charged polyelectrolyte. Addition of kaolin improved the mechanical strength of the beads. Modification of the surface of the beads with PEI facilitated better control of the release rate of the plant growth regulator, phenylacetic acid (PAA). The physical properties of the beads were characterized by optical and scanning electron microscopy (SEM), and their mechanical strength was determined using an Instron® 5565 Tensile Testing Machine. Cumulative release of PAA was measured by UV-Vis spectroscopy.

In the third research project, pectin blended with four other types of anionic polysaccharides, including alginate, carrageenan, xylan and xanthan, were crosslinked with zinc acetate and formed into thin films. In addition, a negatively charged polyelectrolyte, poly(4-styrenesulfonic acid-co-maleic acid) sodium salt (PSSMA) was coated on the film surface with the goal of increasing the capture of cationic contaminants. The average film thickness was measured using a digital micrometer. Surface morphologies and elemental analysis were obtained by energy dispersive spectroscopy connected with scanning electron microscopy. The swelling ratio and the mechanical properties of the films were investigated in relationship to their composition and PSSMA coating. The sorption of model cationic pollutants clearly improved for coated films and showed to be predominantly based on the interaction of positively and negatively charged groups between film/coating and contaminants.

Acknowledgments

Foremost, the author would like to express her heart-felt thanks to her advisor Dr. Gisela Buschle-Diller, for her generous guidance, encouragement, support, patience and valuable advice during her Ph.D study. The author is also very grateful to her committee members, Dr. Maria Auad, Dr. Xinyu Zhang and Dr. Thomas Elder for their precious suggestions and patient guidance to improve her dissertation. The author would especially thank Dr. Thomas Elder and Dr. Mandla Tshabalala for cooperative work and contribution to the research project.

The author gratefully thanks Dr. Ramsis Farag's advise on the mechanical tests, evaluating dissertation and giving suggestions as the University Reader. Thanks also go to Dr. Michael Miller for his help with electron microscopic experiments. The author would also like to thank her group members, Dr. Kai Wang and Dr. Bo Yuan for their teaching, discussion and significant help.

Further, the author would like to thank her parents, Zhigang Li and Huili Mei, and her husband, Teng Wang, for their love, encouragement and support throughout the years.

Table of Contents

List of Tables

List of Figures

List of Abbreviations

NMR	Nuclear magnetic resonance
SEM	Scanning electron microscopic
EDS	Energy dispersive spectroscopy
UV-Vis	Ultraviolet-visible light spectroscopy
MB	Methylene blue
CNC	Nanocrystalline cellulose
PEI	Polyethylenimine
PAA	Phenylacetic acid
PSSMA	Poly(4-styrenesulfonic acid-co-maleic acid)
CV	Crystal violet
CPC	Cetylpyridinium chloride
BtCl	Benzethonium chloride

Chapter 1 Introduction

Polysaccharides

Polysaccharides are naturally occurring, abundant biopolymers, produced by living organisms. They are composed of long chains of monosaccharide units, bound together by glycosidic linkages. Their structure ranges from linear to highly branched. The function of polysaccharides in living organisms is either structure (cellulose and chitin) or storage related (e.g. starch and glycogen). Their physical properties such as solubility, flow behavior, gelling potential and/or surface and interfacial properties, are affected by the type of monosaccharides that make up the polymer, the linkage types and patterns, chain shapes and degrees of polymerization [1]. Important natural polysaccharides include cellulose, alginate, starch, glycogen, chitin, xylan, pectin, carrageenan, xanthan, and many more. The chemical structure of selected polysaccharides is shown in Figure 1.1.

Starch is a neutral polysaccharide produced by most green plants for energy storage. It exists in large amounts in staple foods such as corn (maize), rice, potatoes and wheat. Starch is a white powder with no taste or odor, and it is insoluble in cold water, but its aqueous solution forms a viscous paste at elevated temperature. Starch consist of two types of molecules, linear amylose and branched amylopectin. The ratio of amylose and amylopectin varies according to the botanical origin of the starch and has a significant impact on its properties. For industrial and food applications, starch types are classified according to this ratio. Regular starch contains 20-35% amylose, high amylose starches greater than 40% and waxy starches less than 15% amylose [2]. The amylose/amylopectin ratio and granule size of most common starches are shown in Table 1.1.

Amylose is composed of α-D-glucose units; its unbranched chains allow easy alignment in solution due to their helical structure [3], while the branched amylopectin has a much higher molecular weight and thus considerably impacts the viscosity of a starch solution [4]. Mixing starch with warm water yields a thick paste, which is utilized in many foods but also technical applications such as thickening and stiffening agents. Starch can also be converted into sugars, for instance by malting, and fermented to produce ethanol in the manufacture of beer in the food industry [5] or bioethanol as a transportation fuel. Besides food-related uses, starch has also been used as an adhesive in the papermaking process [6].

Table 1.1 Ratio of amylose/amylopectin and granule size of some common starches [2,7]

Source	Amylose (%)	Amyopectin (%)	Size (μm)
Maize (waxy)	--	100	3−26
Maize (normal)	28	72	2−30
Potato	21	79	5−100
Wheat	26	74	15−35
Rice	20	80	3-8
Tapioca	17	83	5−35

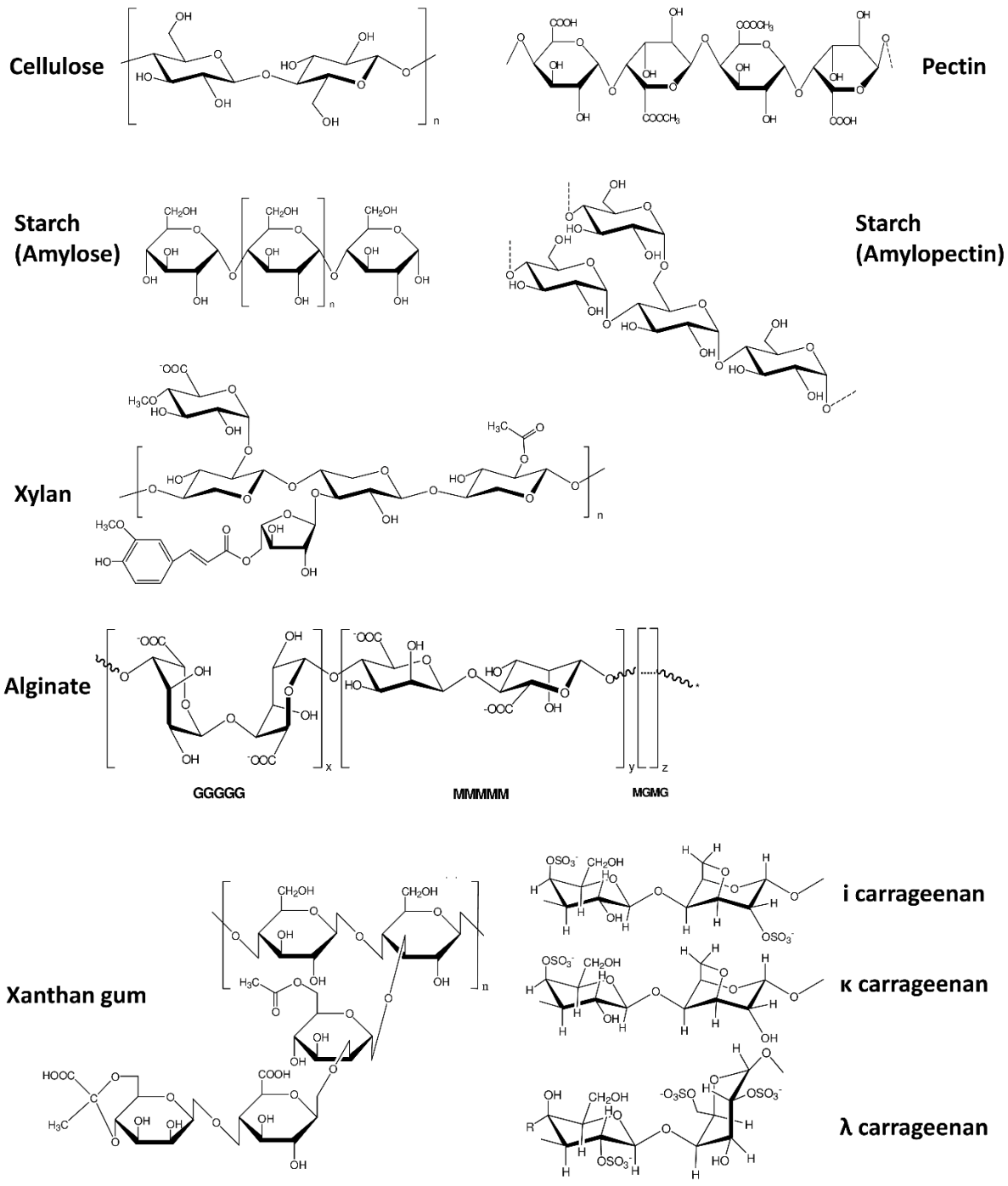

Fig. 1.1 Examples of important polysaccharides.

Cellulose is the most abundant natural polymer on earth [8], since it is the main component of plant cell walls. The linkage in the unbranched cellulose molecule differs from α-glycosidic bonds in glycogen and starch. Here, two glucose units are linked by β-1,4-glycosidic bonds and form cellobiose as the monomeric unit. In cellulose strong hydrogen bonds form between adjacent glucose units, both within a chain and between adjacent chains, creating highly crystalline areas connected by less crystalline, amorphous regions, and organized in a microfibrillar arrangement. This arrangement creates a tougher structure than glycogen and starch and causes cellulose to be insoluble in water and most organic solvents. The amorphous regions can be penetrated and broken down by strong inorganic acids, e.g. H_2SO_4, HCl and HBr as well as by ionic liquids, leaving the crystalline domains as nanofibrillar and nanocrystalline cellulose behind [9-12]. Traditionally, cellulose is an important component of paper, cardboard and textile products as well as countless derivatives in the form of organic and inorganic esters and ethers. Lately, nanocrystalline cellulose has gained increasing attention due to the fact that it can now be produced economically in considerable amounts [9, 11, 13].

Alginate is an anionic, water soluble polysaccharide extracted from the cell walls of brown algae or made by soil bacteria. Chemically, it is a linear copolymer composed of two monomers, (1-4)-linked β-D-mannuronic acid (M) and α-L-guluronic acid (G) residues at different ratios and distribution along the chains [14]. Around neutral pH alginate contains a significant amount of negative charges due to deprotonated carboxylic acid groups. It exhibits a sol-gel transition when sodium counter-ions from G blocks are substituted with divalent ions or multivalent cations, such as calcium, zinc, or barium by forming the “egg-box” structure (Fig. 1.2). Alginate’s ability to form a gel is determined by the proportion and length of G blocks in its molecular structure [15]. The higher the G block content, the greater is its potential to yield a strong gel.

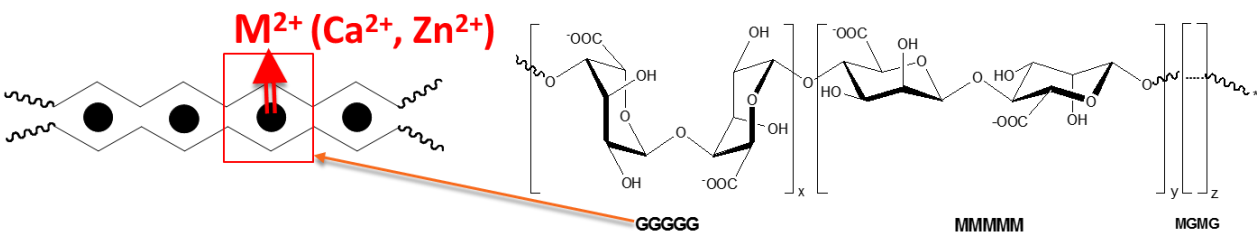

Figure 1.2 “Egg-box” model of crosslinked alginate

Pectin is a structural, anionic polysaccharide produced commercially as a white to light brown powder mainly by extraction from apples or citrus fruits. It is partially soluble in cold water and rich in galacturonic acid. In nature, 80% of carboxyl groups of galaturonic acid are esterified with methanol [16]. However, this proportion can be decreased to a varying degree during pectin extraction. Divalent ions, e.g. Ca^{2+}, Zn^{2+} can react with free carboxyl groups along the pectin chains and form a water-insoluble “egg-box” structure [17-19] which is similar to that of alginate. Pectin is widely used as gelling agent of many food products, especially in jams and jellies. It is also used in fillings, medicines and as stabilizer in fruit juices and milk.

Carrageenan, extracted from red seaweed (*Rhodophycaea*), is an anionic polysaccharide containing sulfate groups along its linear galactose backbone. There are three main types of carrageenan that differ in the number and position of esterified sulfate groups on the repeating galactose units. Among them, kappa-carrageenan has one sulfate group per disaccharide, capable of forming strong and rigid gels with K^+ [20]. Iota-carrageenan with two sulfate groups per disaccharide forms soft gels in the presence of Ca^{2+} [21]. Lambda-carrageenan with three sulfate groups per disaccharide cannot form regular helical structures and thus does not gel. It is mainly used as viscosity builder and thickening agent in dairy products. All three carrageenans are soluble in hot water; only lambda-carrageenan also dissolves in cold water. This is attributed to higher levels of esterification of the sulfate groups and a less ordered structure, thus lowering the

solubility temperature of carrageenan and producing lower strength gels or preventing gel formation altogether.

Xylan is a major component of hemicellulose. It exists in plant cell walls, especially in hardwoods and softwoods, and in some algae. Xylans from different origin differ in composition. Most of the xylans occur as heteropolysaccharides, containing different substituent groups in the backbone and side chains [22, 23] Common groups on the backbone of xylan include acetyl, arabinosyl and glucuronosyl residues [24]. Xylan has been used as adhesive, thickener and additive to polymeric materials. It also shows large potential for packaging films and coating of food, as well as for biomedical products [25].

Xanthan is a polysaccharide commercially produced by fermentation of glucose, sucrose, or lactose with microbial *Xanthomonas campestris* [26]. It is composed of penta-saccharide repeat units, consisting of glucose, mannose and glucurionic acid in a molar ratio of 2:2:1 [27]. Xanthan is soluble in both cold and hot water. It has long been used in the food industry as a thickener in ice-cream, salad dressings and sauces and is now available in many food stores as a replacement for flour. Unlike most starches heat is not necessary for xanthan to hydrate. Thus, it has also been applied as a stabilizer for suspensions, emulsions, foams and solid particles in water-based formulations.

Besides the several neutral and anionic polysaccharides introduced in the above paragraphs, the cationic polysaccharide chitosan has also found broad applications in the past decades. It is commercially produced by deacetylation of chitin, which is the structural element of crustaceans' (such as crabs and shrimp) shells. Its chains contain amino groups with a pK_a value of ~6.5 causing protonation in acidic to neutral solution with a charge density dependent on pH and on the amount

of available amino groups. Protonation of chitosan renders it soluble in water and able to bind with negatively charged surfaces, such as mucosal membranes [28, 29].

Table 1.2 pKa value of ionic groups in polysaccharides [30-33]

	Alginate		Pectin	κ−carrageenan	Xanthan	Xylan	Chitosan
pK_a	3.38 (M)	3.65 (G)	~3.5	~4.9	~3.7	~3.1	~6.5

The pK_a value of several ionic polysaccharides are listed in Table 1.2. Above the pK_a value of each polysaccharide, the ionic functional groups in the polysaccharide start to deprotonate.

Besides the well-known applications of different polysaccharides mentioned above (stabilizers, thickening and gelling agents and encapsulating agent), related work based on their sorption of pollutants and controlled release of agrochemicals will be discussed in the introduction sections of Chapter 2 to Chapter 4.

Adsorption of pollutants from wastewater

Water contamination gives rise to environmental and health concerns and measures must be taken to remove contaminants appropriately. In the following sections, typical pollutants, such as heavy metals, dyes from industrial and consumer discharge as well as cationic antiseptics from pharmaceutical and personal care products are introduced.

Heavy metals exist naturally in the earth but become concentrated as a result of human activities, e.g. mining and industrial use and waste generation, vehicle emissions, lead-acid batteries, paints, and an aging water supply infrastructure. Lead, cadmium, mercury, chromium and arsenic may

leach from industrial operations and consumer water lines and cause pollution of water sources. In addition, acid rain can worsen the pollution by releasing heavy metals trapped in soil [34]. Plants are subjected to heavy metals by chemical treatments which also leach into fresh water supplies. Animals and humans consume these plants. Thus, ingestion of plant and animal based food products are the major sources of heavy metals accumulated in the human body. These heavy metals are able to bind with vital cellular compounds, e.g. structural proteins, enzymes and nucleic acids, thus affect their function [35]. Generally, long term exposure to toxic heavy metals can bring about a series of nervous system and circulatory effects [36].

Dyes have been widely used in many industrial fields, e.g. textiles, paper, plastics, leather and printing. The discharge of dyes wastewater has caused a series of serious environmental pollution problems, such as reducing the light penetration and decreasing the photosynthetic efficiency of aquatic plants. Moreover, most dyes are highly toxic and have mutagenic or carcinogenic influences on aquatic life and human beings even at a low concentration [37]. The chemical structure of four common anionic and cationic dyes are shown in Figure 1.3 as an example.

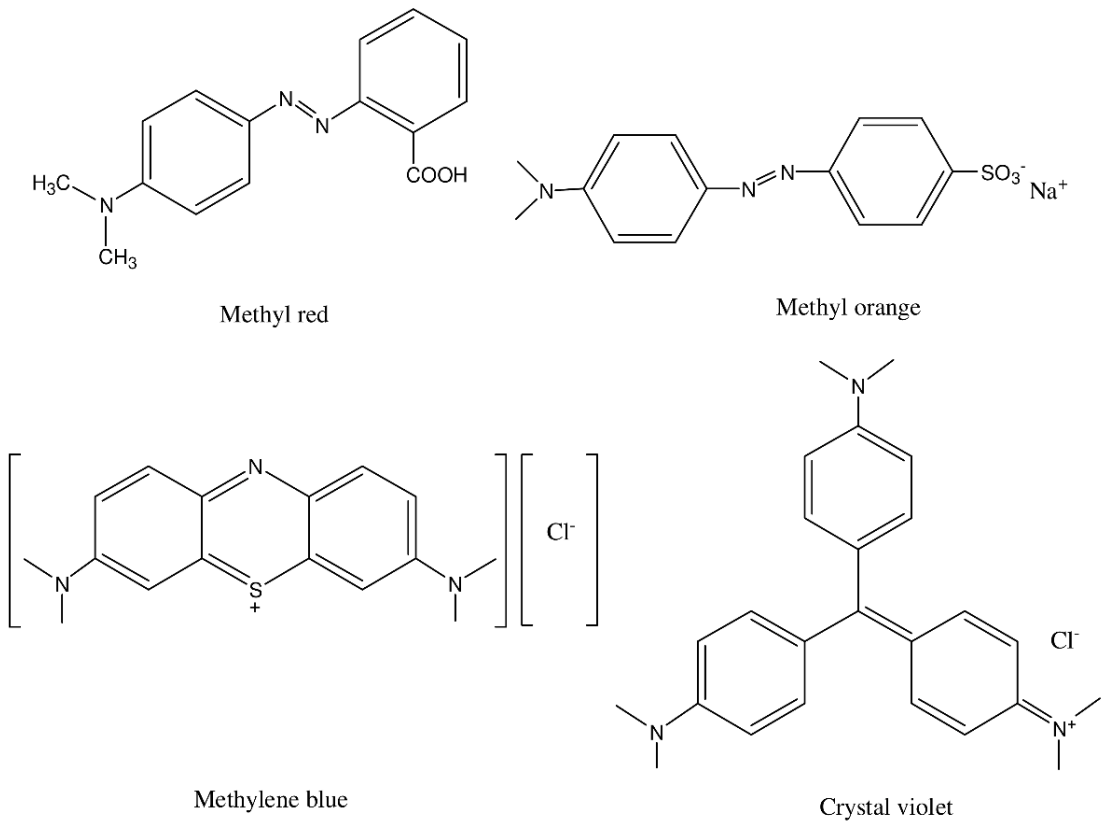

Figure 1.3 Chemical structure of typical cationic dyes

In recent years, pharmaceuticals and personal care product residues have also been detected in water bodies throughout the world [38]. Chemical additives, such as cationic antiseptics commonly used in many types of antimicrobial soaps, mouthwashes and toothpastes, pose potential risks to humans and the aquatic ecosystem, especially when they are released into lakes and rivers and accumulated in higher concentrations. [39, 40]

There are a variety of treatment techniques available, including coagulation, filtration, ion exchange, sedimentation, solvent extraction, adsorption, electrolysis, precipitation, chemical oxidation, etc. [41, 42]. However, there are also numerous shortcomings and limitations to many methods; for example, ion exchange, solvent extraction and chemical oxidation have shown low

efficiency of removal of trace levels of contaminants. Coagulation is pH controlled and the resulting sludge disposal might result in further problems [43]. Among waste water treatment methods, adsorption techniques using fixed bed or trickling filters have become one of the most widely used methods for water remediation. This is attributed to their ease of operation, and the convenience and simplicity of design involved. Depending on the type of the sorbent and filtration set-up, adsorption techniques are capable of simultaneously removing different types of contaminants and/or minimizing their toxic effects [44-46], thus offering a broad application spectrum for water remediation.

On a smaller scale, adsorption is a process based on attraction of atoms, ions or molecules from a gas, liquid or dissolved solid phase to a surface, creating a film or thin layer of the adsorbate on the surface of the adsorbent. The adsorption process is generally categorized into physisorption or physical adsorption and chemisorption. The physisorption is based on weak van der Waals forces while with the chemisorption covalent bonding or ionic bonding can develop. [47] The most common industrial adsorbents include the following three categories:

- Oxygen-containing compounds – mostly hydrophilic and polar compounds, such as silica gels and zeolites.
- Carbon-based compounds – usually hydrophobic and non-polar compounds, including activated carbon and graphite.
- Polymer based compounds – either polar or non-polar compounds with functional groups in a porous polymeric matrix.

A fundamentally important property of effective adsorbents is their high porosity and consequently large surface area with a high number of available adsorption sites. The porous structure not only

impacts surface area and adsorption capacity but also the kinetics of the adsorption. Better adsorbents have larger surface areas and thus require comparatively less time for adsorption to reach equilibrium. Therefore, both a high surface area and faster kinetics for pollutants removal are factors when selecting an adsorbent and both factors not always are equally accessible. In addition, regeneration or disposal of the used filter bed is considerations in addition to the overall cost of the process. In the case of the frequently used activated carbon as sorbent, for example, a large surface area, low density as well as chemical stability are provided [48]. However, the high costs of manufacturing and regeneration make its utilization for large scale wastewater operations uneconomical. Therefore, in recent decades, low cost environmentally-friendly polysaccharide-based materials have attracted increasing attention for the purpose of adsorption of different pollutants. This development will be introduced in more detail in the introduction section of chapter 2 and chapter 4.

Several kinetic models are available to study the mechanisms of the adsorption process in order to fit the experimental data and examine the rate-controlling step in the overall adsorption process. Among them, pseudo-first-order and pseudo-second order models are the most common ones used to describe the adsorption kinetics (Eqs. 1.1 and 1.2 [49, 50]).

Pseudo-first-order model

$$\log (q_e - q_t) = \log q_e - \frac{k_1}{2.303} t \qquad \text{(Equation 1.1)}$$

q_e and q_t are the amounts of cationic compounds adsorbed (mg g^{-1}) at equilibrium and at time t (min), k_1 is pseudo-first-order rate constant (min^{-1})

Pseudo-second-order model

$$\frac{dq_t}{q_t} = k_2(q_e - q_t)^2 \qquad \text{(Equation 1.2)}$$

Where q_e and q_t are the amounts of cationic compounds adsorbed (mg g^{-1}) at equilibrium and at time t (min), k_2 (g mg^{-1} min^{-1}) is the rate constant of the pseudo-second-order reaction. After integrating this equation with the boundary conditions t=0 (q_t=0) to t_e (q_t=q_e), it then is linearized into Equation 1.3.

$$\frac{t}{q_t} = \frac{1}{k_2 q_e^{\,2}} + \frac{t}{q_e} \qquad \text{(Equation 1.3)}$$

Where constant k_2 and q_e values were calculated from the slope and intercepts of the t/qt versus t plot.

The purpose of these models is to determine the maximum adsorption capacity at equilibrium as well as the adsorption kinetics rate constants (k_1 and k_2). A higher value of the rate constant reflects a faster removal of the pollutant from the solution and a better adsorbent. q_e calculated from the kinetic model shows the potential amount of removal of pollutant by a given adsorbent. Thus, q_e is also associated with the efficiency of the adsorbent.

Controlled release formulation of agrochemicals

Many sorbent compounds can also reversely serve as release systems for active compounds due to the properties mentioned in the previous sections (high surface area, porous system). Release characteristics are also important for regeneration purposes.

Conventional release formulations usually fall below the efficient level after an initial burst release. With compounds functioning as controlled release vehicles, a continuous and stable release of active ingredients can be achieved from the carrier into a target medium, maintaining a

predetermined minimum effective level for a specified period of time. It is therefore not surprising, that such compounds have found a wide range of applications in many areas including the pharmaceutical, cosmetic, personal care, agricultural and food industries [51-53].

Agrochemicals are a category of chemicals used widely in agriculture. They include the broad range of pesticides, e.g. insecticides and fungicides. They also include herbicides, fertilizers, hormones and other chemical growth agents. Some of these biologically active chemicals have been very effective in suppressing undesirable weeds and insects (pesticides and herbicides) and some of them improve the growth of crops (plant hormones), thereby reaching the goal of increasing food production for a growing population. For instance, plant hormones regulate the cellular processes in targeted cells locally and move to other functional parts of the plant. They also are instrumental in the formation of flowers, stems, leaves, shedding of leaves, and the development and ripening of fruit [54]. These hormones are absolutely vital to plant growth.

Conversely, the application of such bioactive chemicals should not create any adverse effects on human health and the environment. Generally, the life span of an active compound adds an important factor to the equation. For example, the use of DDT (dichlorodiphenyltrichloroethane), a pesticide with a very long life span is undesirable since its residues enter the food chain and pose serious dangers to human health [55]. On the other hand, these active chemicals with very short life span do not serve the purpose as they are susceptible to be washed away by rain water, removed by evaporation or rapidly biodegraded into inactive components. In recent years, over two million tons of pesticides were applied to control pathogens and pests every year all over the world. However, around 90% of the pesticides are actually lost due to their degradation, photolysis, evaporation and surface runoff, and only a very small percentage of the pesticides are actually

deposited on their biological targets [56, 57]. The long-term extensive and insufficient use of these agrochemicals has caused serious concerns regarding food safety and the ecological well-being of the environment [58]. Therefore, an efficient way to improve the utilization of agrochemicals via prolonged effectiveness with simultaneously reduced application time and dosage is needed.

Controlled release of agrochemicals could be one way to achieve a more economic, safe and effective insect control and plant growth, as well as reduced environmental pollution. Polysaccharides provide a safe vehicle to accomplish this goal. A schematic of a potential polysaccharide system is shown in Figure 1.4. As with sorption of pollutants, mathematical models can provide insights into the mechanism and the reaction kinetics of the delivery of active compounds from a matrix.

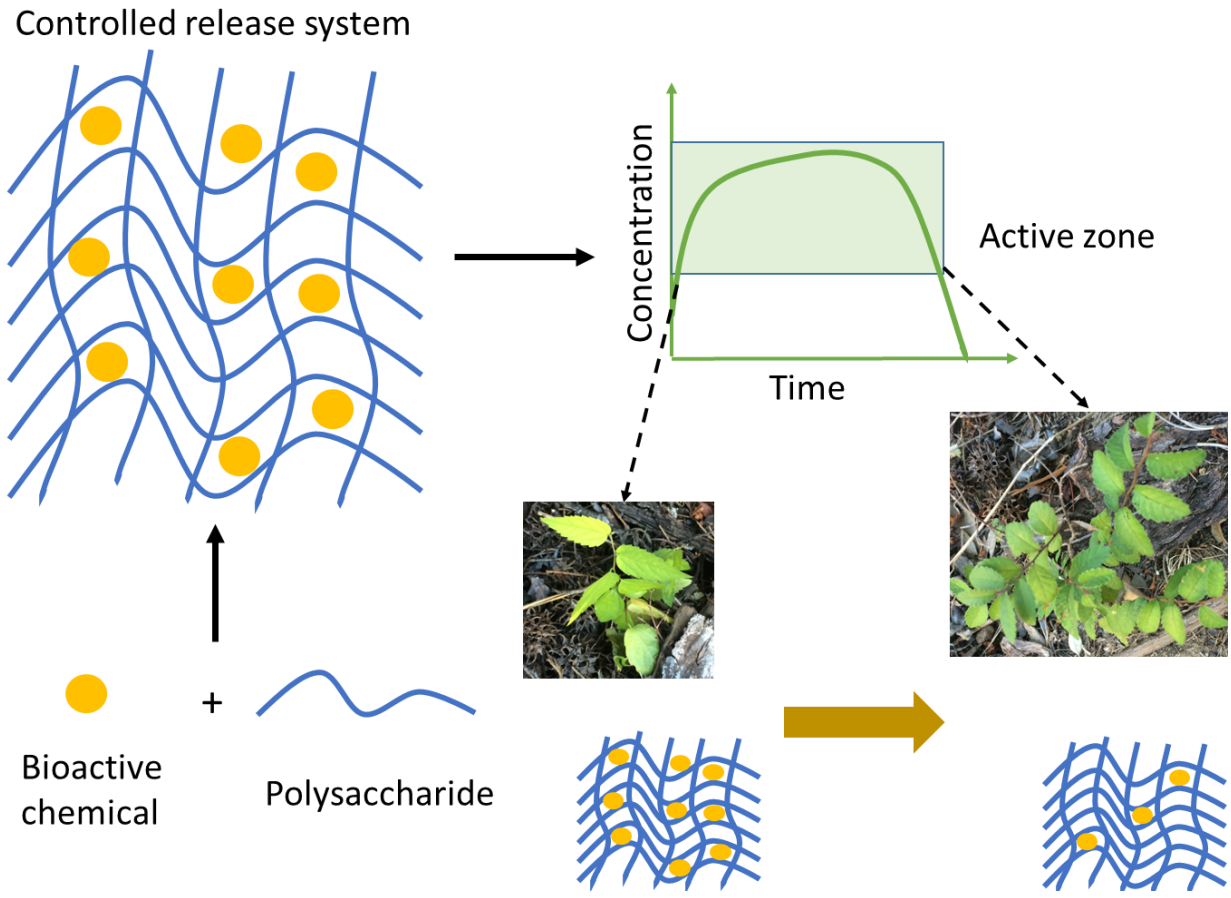

Figure 1.4 A representation of delivery system based on polysaccharides for bioactive chemicals (an example for plant growth factors) targeting applications in agriculture.

Zero-order release kinetics [59] refers to the ideal process of constant chemical release from a chemical delivery matrix that is independent on the concentration. Its simplest form can be expressed as (Eq. 1.4):

$$Q = Q_0 + k_0 t \quad \text{(Equation 1.4)}$$

where Q is the amount of chemical released, Q_0 is the initial amount of chemical in solution (usually it is zero) and k_0 is the zero order release constant.

First-order release kinetics

The earliest model expressing dissolution rate in a quantitative manner was proposed by Noyes and Whitney (Eqs. 1.5 and 1.6, [60]) as:

$$-dC/dt = k(C_s - C_t) \quad \text{(Equation 1.5)}$$

where dC/dt is the rate of change in concentration with time, k is the rate constant. The integrated form of the above equation is:

$$\log C = \log C_0 - k_1 t/2.303 \quad \text{(Equation 1.6)}$$

where C_0 is the initial concentration of chemical and k_1 is the first order release constant. This equation predicts a first order dependence on the concentration gradient (e.g. $C_s - C_t$) between the static liquid layer next to the solid surface and bulk liquid. Noyes and Whitney explained their dissolution data using a concept similar to that used for the diffusion model. These considerations relate to the conditions where there is no change in the shape of the solid during the dissolution process (e.g. the surface area remains constant). However, for some matrices, swelling occurs during the dissolution process and the surface area changes over a period of time.

The Hixson-Crowell cube root law describes the release from systems where there is a change in surface area and diameter of the release matrix [61]. The relationship can be expressed as shown in Eq. 1.7:

$$Q_0^{1/3} - Q_t^{1/3} = k_{HC}\, t \qquad \text{(Equation 1.7)}$$

Where Q_t is the amount of chemical released (cumulative % release) in time t, Q_0 is the initial amount of chemical in matrix and k_{HC} is the rate constant for Hixson-Crowell rate equation.

Many controlled release products are designed on the principle of embedding the chemical in a porous matrix. When liquid penetrates the matrix and dissolves the drug, the chemical diffuses into the exterior liquid. Higuchi [62] was the first to derive an equation to show the release of a chemical from an insoluble matrix as the square root of a time-dependent process simplified as in Eq. 1.8:

$$Q_t = k_H\, (t)^{0.5} \qquad \text{(Equation 1.8)}$$

Q_t is the amount of chemical released (cumulative % release) in time t and k_H is the release rate constant for the Higuchi model. k_H is related to several factors, including the diffusion coefficient, solubility of chemical in dissolution media, porosity (the fraction of matrix that exists as pores or channels into which the surrounding liquid can penetrate), tortuosity (the path length of diffusion caused by branching and bending of the pores) and chemical content per cm^3 of matrix.

The Korsmeyer-Peppas model [63] is a model mostly used to describe chemical release from a polymeric system with cylindrical pores (Eq. 1.9).

$$M_t/M_\infty = kt^n \qquad \text{(Equation 1.9)}$$

M_t/M_∞ is the fraction of chemical released at time t, k is the rate constant and n is the release exponent. The value of n reflects different mechanisms, when n=0.45, the diffusion mechanism

is Fickian diffusion. When $0.45<n<0.89$，the transport mechanism is Non-Fickian and n=0.89 refers to Case II transport. If n>0.89, the diffusion mechanism is referred to as Super case-II transport.

References

[1]. Mano JF, Silva GA, Azevedo HS, Malafaya PB, Sousa RA, Silva SS, Boesel LF, Oliveira JM, Santos TC, Marques AP, Neves NM, Reis RL (2007) Natural origin biodegradable systems in tissue engineering and regenerative medicine: present status and some moving trends, J R Soc Interface 4: 999-1030

[2]. Tester RF, Karkalas J, Qi X (2004) Starch-composition, fine structure and architecture, J Cereal Sci 39: 151-165

[3]. McGrane SJ, Mainwaring DE, Cornell HJ, Rix CJ (2004) The role of hydrogen bonding in amylose gelation, Starch 56: 122-131

[4]. Hermansson AM, Svegmark K (1996) Developments in the understanding of starch functionality, Trends Food Sci Tech 7: 345-353

[5]. Sharma SK, Mudhoo A, Clark JH (2011) A handbook of applied biopolymer technology: synthesis, degradation and application, Royal society of chemistry

[6]. Burrell MM (2002) Starch: the need for improved quality or quantity-an overview, J Exp Bot 54: 451-456

[7]. Hegenbart S (1996) Understanding starch functionality-natural food insider, http://www.naturalproductsinsider.com/articles/1996/01/understanding-starch-functionality.aspx

[8]. Anderson JW, Baird P, Davis RH Jr, Ferreri S, Knudtson M, Koraym A, Waters V, Williams CL (2009) Health benefits of dietary fiber, Nutr Rev 67: 188-205

[9]. Battista OA (1950) Hydrolysis and crystallization of cellulose, Ind Eng Chem 42: 502-507

[10]. Roman M, Winter WT (2004) Effect of sulfate groups from sulfuric acid hydrolysis on the thermal degradation behavior of bacterial cellulose, Biomacromolecules 5: 1671-1677

[11]. Sadeghifar H, Filpponen I, Clarke SP, Brougham DF, Argyropoulos DS (2011) Production of cellulose nanocrystals using hydrobromic acid and click reactions on their surface, J Mater Sci 46: 7344-7355

[12]. Zhang Z, Zhao ZK (2009) Solid acid and microwave-assisted hydrolysis of cellulose in ionic liquid, Carbohyr Res 344: 2069-2072

[13]. Peng BL, Dhar N, Liu HL, Tam KC (2011) Chemistry and applications of nanocrystalline cellulose and its derivatives: A nanotechnology perspective, Can J Chem Eng 89: 1191-1206

[14]. Robitzer M, David L, Rochas C, Renzo FD, Quignard F (2008) Nanostructure of calcium alginate aerogels obtained from multistep solvent exchange route. Langmuir 24: 12547-12552

[15]. Lee KY, Mooney DJ (2012) Alginate: properties and biomedical applications, Prog Polym Sci 37: 106-126

[16]. Sriamomsak P (2003) Chemistry of pectin and its pharmaceutical uses: A review, Silpakorn University Int J 3: 206-228

[17]. Dupuis G, Chambin O, Genelot C, Champion D, Pourcelot Y (2008) Colonic drug delivery: influence of cross-linking agent on pectin beads properties and role of the shell capsule type, Drug Dev Ind Pharm 32: 847-855

[18]. El-Gibaly I (2002) Oral delay-release system based on Zn-pectinate gel (ZPG) microparticles as an alternative carrier to calcium pectinate beads for colonic drug delivery, Int J Pharm 232: 199-211

[19]. Alvarez-Lorenzo C, Blanco-Fernandez B, Puga AM, Concheiro A (2013) Crosslinked ionic polysaccharides for stimuli-sensitive drug delivery, Adv Drug Deliv Rev 65: 1148-1171

[20]. Yuguchi Y, Thuy TTT, Urakawa H, Kajiwara K (2002) Structural characteristics of carageenan gels: temperature and concentration dependence, Food Hydrocolloid, 16: 515-522

[21]. Thrimawithana TR, Young S, Dunstan DE, Alany RG (2010) Texture and rheological characterization of kappa and iota carrageenan in the presence of counter ions, Carbohyd Polym 82: 69-77

[22]. Biely P (1985) Microbial xylanolytic systems, Trends Biotechnol 3: 286-290

[23]. Puls J, Poutanen K (1989) Mechanisms of enzymatic hydrolysis of hemicelluloses (xylans) and procedures for determination of the enzyme activities involved, Enzyme systems for lignocellulose degradation, 151-165

[24]. Whistler RL, Richards EL (1970) Hemicellulose, Carbohyd 2: 447-469

[25]. Li X, Shi X, Wang M, Du Y (2011) Xylan chitosan conjugate-A potential food preservative, Food Chem 126: 520-525

[26]. Barrere GC, Barber CE, Daniels MJ (1986) Molecular cloning of genes involved in the production of the extracellular polysaccharide xanthan by *Xanthomonas campestris* pv. *campestris*, Intl J Biol Macromolec 8: 372-374

[27]. Garcia-Ochoa F, Santos VE, Casas JA, Gomez E (2000) Xanthan gum: production, recovery, and properties, Biotechnol Adv 18: 549-579

[28]. Lee DW, Lim C, Israelachvili JN, Hwang DS (2013) Strong adhesión and cohesion of chitosan in aqueous, Langmuir, 29: 14222-14229

[29]. Lim C, Lee DW, Israelachvili JN, Jho Y, Hwang DS (2015) Contact time- and pH-dependent adhesión and cohesion of low molecular weight chitosan coated surfaces, Carbohyd Polym 117:

887-894

[30]. Sadeghi M (2012) Synthesis of a biocopolymer carrageenan-g-poly(AAm-co-IA)/montmorilonite superabsorbent hidrogel composite, Braz J Chem Eng, 29: 295-305

[31]. Teleman A, Harjunpaa V, Tenkanen M, Buchert J, Hausalo T, Drakenberg T, Vuorinen T (1995) Characterisation of 4-deoxy-beta-L-threo-hex-4-enopyranosyluronic acid attached to xylan in pine kraft pulp and pulping liquor by 1H and 13C NMR spectroscopy, Carbohyr Res, 272: 55-71

[32]. Opanasopit P, Apirakaramwong A, Ngawhirunpat T, Rojanarata T, Ruktanonchai U (2008) Development and characterization of pectinate micro/nanoparticles for gene delivery, AAPS PharmSciTech 9: 67-74

[33]. Simsek-Ege FA, Bond GM, Stringer J (2003) Polyelectrolyte complex formation between alginate and chitosan as a function of pH, J Appl Polym Sci 88: 346-351

[34]. Wuana RA, Okieimen FE (2011) Heavy metals in contaminated soils: A review of sources, chemistry risks and best available strategies for remediation, ISRN Ecology 2011, http://dx.doi.org/10.5402/2011/402647

[35]. Jarup L (2003) Hazards of heavy metal contamination, Br Med Bull 68: 167-182

[36]. Jaishankar M, Tseten T, Anbalagan N, Mathew BB, Beeregowda KN (2014) Toxicity, mechanism and health effects of some heavy metals, Interdiscip Toxicol 7: 60-72

[37]. Forgacs E, Cserhati T, Oros G (2004) Removal of synthetic dyes from wastewaters: A review, Environ Int 30: 953-971

[38]. Sui Q, Cao X, Lu S, Zhao W, Qiu Z, Yu G (2015) Occurrence, sources and fate of pharmaceuticals and personal care products in the groundwater: A review, Emerging Contaminants 1: 14-24

[39]. Segura PA, Francois M, Gagnon C, Sauve S (2009) Review of the occurrence of anti-infectives in contaminated wastewaters and natural and drinking water, Environ Health Perspect 117: 675-684

[40]. Carvalho IT, Santos L (2016) Antibiotics in the aquatic envionments: A review of the European scenario, Environ Int 94: 736-757

[41]. Vandevivere PC, Bianchi R, Verstraete W (1998) Review: Treatment and reuse of wastewater from the textile wet-processing industry: Review of emerging technologies, J Chem Technol Biotechnol 72:289-302

[42]. Sonune A, Ghate R (2004) Developments in wastewater treatment methods, Desalination 167: 55-63

[43]. Barakat MA (2011) New trends in removing heavy metals from industrial wastewater, Arab J Chem 4: 361-377

[44]. Bradl HB (2004) Adsorption of heavy metal ions on soils and soils constituents, J Colloid Interface Sci 277: 1-18

[45]. Yagub MT, Sen TK, Afroze S, Ang HM (2014) Dye and its removal from aqueous solution by adsorption: A review, Adv Colloid Interface Sci 209: 172-184

[46]. Karanfil T, Kilduff JE (1999) Role of Granular Activated Carbon Surface Chemistry on the Adsorption of Organic Compounds. 1. Priority Pollutants, Environ Sci Technol 33: 3217-3224

[47]. Ferrari L, Kaufmann J, Winnefeld F, Plank J (2010) Interaction of cement model systems with superplasticizers investigated by atomic force microscopy, zeta potential, and adsorption measurements J Colloid Interface Sci. 347 (1): 15–24

[48]. Bansal RC, Goyal M (2005) Activated carbon adsorption, CRC press

[49]. Yuh-Shan H (2004) Citation review of Lagergren kinetic rate equation on adsorption reactions, Scientometrics 59: 171-177

[50]. Ho YS, Mckay G (1999) Pseudo-second order model for sorption processes, Process Biochem 34: 451-465

[51]. Gerstl Z, Nasser A, Mingelgrin U (1998) Controlled reléase of pesticides into soils from clay-polymer formulations, Inst Soil Water Environ Sci 46: 3797-3802

[52]. Gupta P, Vermani K, Garg S (2002) Hydrogels: from controlled release to pH-responsive drug delivery, Drug Discov Today 7: 569-579

[53]. Langer R, Peppas N (1983) Chemical and physical structure of polymers as carriers for controlled release of bioactive agents: A review, J Macromol Sci C 23: 61-126

[54]. Luckwill LC (1953) Studies of fruit development in relation to plant hormones: II. The effect of naphthalene acetic acid on fruit set and fruit development in apples, J Hortic Sci 28:25-40

[55]. Walker CH, Sibly RM, Hopkin SP, Peakall DB (2012) Prinic ecotoxicol, CRC press

[56]. Li ZZ, Xu SA, Wen LX, Liu F, Liu AQ, Wang Q, Sun HY, Yu W (2006) Controlled release of avermectin from porous hollow silica nanoparticles: Influence of shell thickness on loading efficiency, UV-shielding property and release, J Control Release 111:81-88

[57]. Ghormade V, Deshpande MV, Paknikar KM (2011) Perspectives for nano-biotechnology enabled protection and nutrition of plants, Biotechnol Adv 29: 792-803

[58]. Pimentel D, Acquay H, Biltonen M, Rice P, Silva M, Nelson J, Lipner V, Giordano S, Horowitz A, D'Amore M (1992) Envionmental and economic costs of pesticide use, BioScience 42: 750-760

[59]. Hsieh DST, Rhine WD, Langer R (1983) Zero-order controlled-release polymer matrices for micro- and macromolecules, J Pharm Sci 72: 17-22

[60]. Schwartz JB, Simonelli AP, Higuchi WI (1968) Drug release from wax matrices I. Analysis of data with first-order kinetics and with the diffusion-controlled model, J Pharm Sci 57: 274-277

[61]. Hixson AW, Crowell JH (1931) Dependence of reaction velocity upon surface and agitation, Ind Eng Chem, 23: 1160-1168

[62]. Higuchi T (1963) Mechanism of sustained-action medication. Theoretical analysis of rate of release of solid drugs dispersed in solid matrices, J Pharm Sci 52:1145-1149

[63]. Korsmeyer RW, Gurny R, Doelker E, Buri P, Peppas NA (1983) Mechanisms of solute release from porous hydrophilic polymers, Int J Pharm 15: 25-35

Objective

This dissertation consists of three projects. The overall goal of this research was to create beads and films from polysaccharide systems crosslinked with Ca^{2+} and Zn^{2+} and equipped with a coating for the targeted removal of cationic contaminants from water (Chapters 2 and 4) and for the controlled release of an anionic plant hormone (Chapter 3). It was explored if both a kaolin filler and a positively charged polyelectrolyte as surface coating showed improved mechanical strength of the polysaccharide beads and better retardation of anionic active compound release (Chapter 3). The approach of Chapter 4 was to incorporate a negatively charged polyelectrolyte as surface coating on pectin-based films for enhanced sorption of cationic pollutants.

Chapter arrangement

This dissertation is organized in four chapters. Chapter 1 presents the overall introduction to the topics of the related research area. Chapters 2 to 4 are the major body of each project in the

sequence of alginate-based beads for cationic contaminants removal, controlled release of agrochemicals from alginate-based beads, and pectin-based films for sorption of cationic compounds from water. Each chapter includes an introduction, experimental details, results and discussion, conclusion and references section.

Chapter 2 Alginate-based polysaccharide beads for cationic contaminant sorption from water

2.1 Introduction

Water contamination is a very severe global environmental problem. Although much research has been focused on water purification, many challenges still remain. Agricultural run-off, by-products of pulp and paper, textile and food industries are major contributors to the problem [1]. Heavy metals, nitrates, pesticides, fertilizers and other chemicals are among the most persistent hazardous contaminants that demand highly efficient treatment processes. At the same time these measures must be cost-effective and affordable in all countries, but especially in those with low economic development [2].

Alginic acid is a naturally abundant polysaccharide extracted from brown algae and soil bacteria. Chemically, it is a linear copolymer composed of two monomers, (1-4)-linked β-D-mannuronic acid (M) and α-L-guluronic acid (G) residues at different ratios and distribution along the chains [3]. Around neutral pH alginate contains a significant amount of negative charges due to deprotonated carboxylic acid groups. These negative charges enable alginate to induce repulsive electrostatic forces and to swell as well as to interact with positively charged ionic groups. Sodium alginate exhibits a sol-gel transition when sodium counter-ions are substituted with divalent cations, such as calcium, zinc, or barium.

Beads made from alginic acid salts have been found to be suitable as a supporting matrix for cell immobilization and drug encapsulation as documented in numerous publications [4-15]. For instance, calcium-crosslinked alginate beads were used as preliminary material for matrices in

enzyme immobilization. Zhu et al. [4] encapsulated glucose oxidase in alginate microspheres; Ai et al. [5] incorporated boehmite into alginate, forming hybrid beads for enhanced enzyme loading. Furthermore, some researchers found that fungal biomass could be entrapped in alginate beads which improved the removal of specific metal ions or dyes. For instance, Torres et al. [6] prepared calcium alginate beads to target the removal of gold and silver. Live and heat inactived fungal mycelia of *Phanerochaete chrysosporium* were employed to bind mercury, lead, cadmium and other metals [7, 8]. Live and dead *Lentinus sajor-caju* [9] were entrapped into alginate beads for increased Hg(II), Zn(II) and Pb(II) removal from waste water. Biosorption of the metal ions occurred within a short time frame and at an astonishingly high yield.

Besides heavy metals, dyes are a serious problem in waste water treatment, since colorants do not easily decompose. Elzatahry et al. [10] used a dynamic batch process to investigate the efficiency of methylene blue removal from colored effluents by alginate micro beads. Extensive research has been performed on biosorption of metals and proteins as well as basic dyes from effluent of the leather industry by Aravindhan et al. [11, 12] using different types of sorbents. Sorption isotherms have been determined for the different sorbent/pollutant systems. Chitosan, a positively charged polysaccharide, can be applied as a surface layer on the outside of alginate beads to reinforce the beads' properties and removal capacity of heavy metal ions and dyes.

A number of publications focused on the performance of magnetic alginate beads [13, 14] for use in cationic dye removal. Magnetism and sorption properties were provided through the combination of active carbon and magnetic nanoparticles which made it possible to recover the beads in a magnetic field. Halloysite nanotubes, a well-known material for removal of various organic pollutants and metal ions, were incorporated to create a new kind of bead with high

porosity according to the work reported by Liu et al. [15]. However, many natural, abundant and biodegradable polysaccharides such as starch, cellulose and xylan also have potential to improve the capacity of waste water remediation and controlled release of chemicals, such as plant hormones [16]. They have not yet been investigated in alginate composite beads to a large extent with the exception of alginate-chitosan combinations.

The work described here is concerned with preparing a series of polysaccharide blended beads composed of alginate and an additional polysaccharide (starch, xylan, cellulose powder and nanocrystalline cellulose) with the goal of influencing internal and external surface properties and swelling/sorption behavior. The average size and size distribution in air/freeze dry state, the swelling ratios, and the morphologies of the resulting beads were studied. The maximum charge density that the beads can acquire and the amount of bound and free water at different moisture contents using low-field NMR spectroscopy were also investigated. In addition, the sorption capacity for a cationic model dye - methylene blue - was assessed and was found to be affected by several factors, including drying methods and pH of crosslinking at the bead formation stage. The admixture of the additional polysaccharide component proved to be a key factor affecting morphology, porosity and sorption sites of the beads for cationic compounds.

2.2 Experimental

2.2.1 Materials

Alginic acid sodium salt from brown algae (medium viscosity, M_w 80000-120000, M/G ratio of 1.56), cellulose (Avicel powder, ~20 micron), xylan from beechwood (M_w~21000), and methylene blue (MB) were purchased from Sigma Aldrich. Nanocrystalline cellulose (CNC) was provided

by the U.S. Department of Agriculture, Forest Products Laboratory, Madison, WI. Unmodified regular food grade corn starch (M_w 10^6-10^7; approx.27% amylose), sodium hydroxide solution (0.0498-0.0502 N), hydrochloric acid (0.1 N) and potassium chloride were obtained from Thermo Fisher, and calcium chloride from Merck. All materials were used as received.

2.2.2 Preparation of polysaccharide beads

A series of homogenous aqueous suspensions were prepared by mixing 2% w/v aqueous sodium alginate with corn starch, cellulose powder, nanocrystalline cellulose, or xylan (all in powder form) with stirring at room temperature. Concentrations of corn starch and cellulose powder were 1, 3, 5 or 10% w/v, while the concentrations of xylan were 1 and 3%, and nanocrystalline cellulose 1% w/v. The suspensions were added to 0.2 M calcium chloride solution as the crosslinking agent through a 10 mL syringe with a needle size of 18G×$1^1/_2$ to form spherical beads at a rate of 4 mL/min. The beads were allowed to crosslink for additional 30 min with gentle stirring. Finally, they were rinsed with distilled water and dried (air-drying or freeze-drying) or used freshly made without drying in the case of methylene blue sorption experiments.

2.2.3 Size measurement of beads

Optical microscopy was used to measure the sizes of both air-dried and freeze-dried beads. 20 beads within each sample and three diameters for each bead (maximum, minimum and diagonal) were measured and the average diameter was recorded.

2.2.4 Swelling ratios of beads

Defined amounts of wet beads obtained directly from synthesis were dried to equilibrium by either

air-drying or freeze-drying. The average weight of the dried beads was determined and the beads immersed in distilled water for 48 h. The swelling ratio was calculated based on the formula shown in Equation 2.1.

$$\text{Swelling ratio } \% = \frac{W_s - W_d}{W_d} \times 100\% \qquad \text{(Equation 2.1)}$$

where W_s is the weight of the water-swollen beads, and W_d the weight of the dried beads.

2.2.5 NMR measurements

Low-field, nuclear magnetic resonance experiments were done using a Bruker mq20 NMR Analyzer with a 0.7 T magnet, operating at 20 MHz and 40°C. The CPMG (Carr-Purcell-Meiboom-Gill) pulse sequence was used with a pulse separation of 5 ms, the collection of 1000 echoes, 64 scans, and a 5 second recycle delay. T2 distributions were determined using Contin [17]. Samples were prepared by saturating ~1 g of air dry and freeze dried beads overnight in 3 mL of deionized water.

2.2.6 Scanning electron microscopic (SEM) analysis of beads

The surface morphology of air-dried and freeze-dried beads as well as morphologies of their cross sections were observed by scanning electron microscopy (SEM) at a 20kV accelerating voltage and working distance 8.5-17mm, using a Zeiss EVO 50 Variable Pressure SEM. The samples were sputter-coated with gold in an EMS 550X Auto Sputter Coating Device.

2.2.7 Charge density of suspensions with different composition

The charge density of suspensions in meq g^{-1} of alginate of different compositions was determined

according to published procedures for direct potentiometric titration of natural organic matter (NOM) [18]. A homogenous mixture was prepared by adding 0.1 M KCl solution into 20 mL of a suspension composed of 2% w/v alginic acid sodium salt solution containing 1% of corn starch, nanocrystalline cellulose and cellulose powder, respectively. These solutions were titrated starting at pH 7.4 (initial pH of suspension). 2% w/v alginic acid sodium salt with 1% xylan had an initial pH of 5.4. Therefore, a second alginate control solution was adjusted to pH 5.4 by adding 0.03N hydrochloric acid. The mixture was titrated with 0.02 N NaOH solution. NaOH solution was added in 0.2 mL increments or its integral multiple; the pH was recorded after each addition of titrant. All samples were titrated up to approximately pH 11. The titrations were performed four times and the values averaged. The charge density of alginate was calculated based on pH measurements and the charge balance of solution calculated as shown in Equation 3.2:

$$\text{Charge density (meq g}^{-1}\text{ alginate)} = \frac{[H^+] + [Na^+] - [OH^-]}{C_{alginate}} \qquad \text{(Equation 2.2)}$$

The concentrations of H^+, Na^+ and OH^- are recorded in meq mL^{-1} and $C_{alginate}$ in g mL^{-1}. Potassium and chloride were not taken into account in the charge balance as they were opposite in charge and equal in concentration.

2.2.8 Capacity of beads to adsorb methylene blue (MB) in aqueous solution

The sorption capacity of the beads for a cationic compound (MB) was investigated with two types of freshly made wet beads (10 g wet weight; crosslinked with $CaCl_2$ solutions at pH 9 and at pH 11, respectively). The beads were added to 50 mL aqueous MB solution of an initial concentration of 5 mg L^{-1}. Additionally, two types of dried beads were investigated: 0.5 g air-dried and 0.5 g freeze-dried beads, respectively, were placed into 30 mL MB solution each (2 mg L^{-1}). In order to

determine unknown concentrations of MB solutions, a calibration curve was created by UV-Vis measurements from a standard MB solution series with known concentrations. Readings were taken at intervals of 15 min until equilibrium was reached. The formula used to calculate the sorption capacity is given in Equation 3.3.

$$\text{Sorption Capacity } q = \frac{(C_0 - C) \times V}{m} \qquad \text{(Equation 2.3)}$$

V signifies the volume of MB solution in mL; C_0 the initial MB concentration in mg L^{-1}; C the MB concentration at intervals of 15 min (mg L^{-1}); and m the weight of the dried beads in g.

2.2.9 Sorption kinetics

Several mathematical theories in modeling the sorption kinetics of pollutants are available; among them, pseudo-first-order and pseudo-second order kinetics are the most important and commonly used ones. [19] The sorption kinetics can be described by pseudo-first-order (Eq. 2.4) or pseudo-second-order (Eq.2.5). To determine which model better reflects the sorption behavior of the beads, the experimental sorption capacity and the parameters of MB were fitted to both kinetic models.

Pseudo-first-order kinetic model

$$\log (q_e - q_t) = \log q_e - \frac{k_1}{2.303} t \qquad \text{(Equation 2.4)}$$

q_e and q_t are the amounts of cationic compounds sorbed (mg g^{-1}) at equilibrium and at time t (min), k_1 is pseudo-first-order rate constant (min^{-1})

Pseudo-second-order kinetic model

$$\frac{t}{q_t} = \frac{1}{k_2 q_e^{\,2}} + \frac{t}{q_e} \qquad \text{(Equation 2.5)}$$

q_e and q_t are the amounts of cationic compounds sorbed (mg g^{-1}) at equilibrium and at time t (min), k_2 (g mg^{-1} min^{-1}) is the rate constant of pseudo-second-order.

2.3 Results and Discussion

2.3.1 Size and size distribution of beads

The average diameter of air-dried beads formed with alginate and alginate blends is shown in Fig. 2.1a. As can be seen, the average size of blended polysaccharide beads only slightly differed from alginate alone at low admixture concentrations. Within the same series, beads were noticeably larger for higher percentages (5 and 10% starch and cellulose powder, respectively). CNC could not be homogenously distributed in alginate at concentrations above 1% and xylan above 3%. Therefore, experiments were limited to lower admixture concentrations of CNC and xylan.

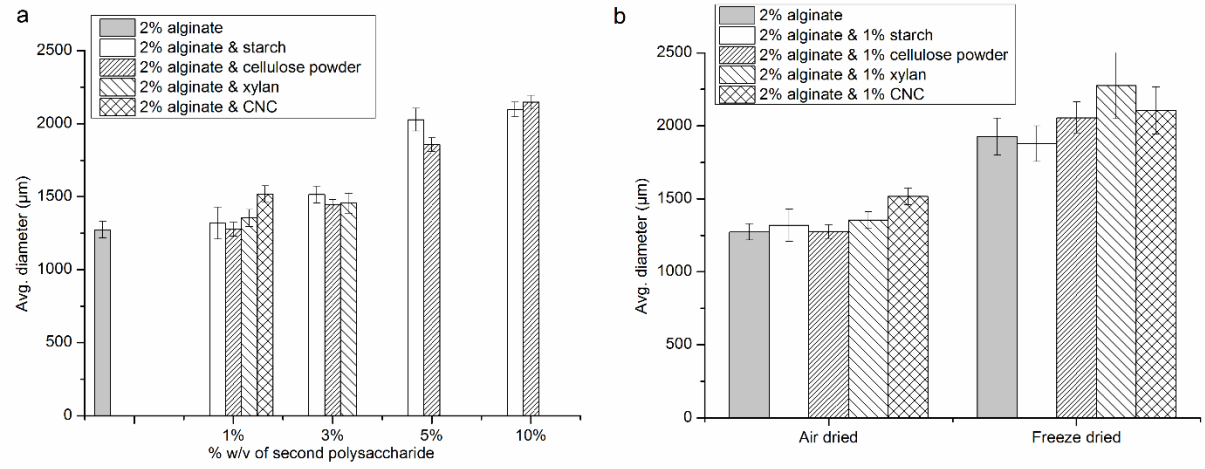

Fig. 2.1 Average diameters of (a) air-dried alginate beads of different composition, (b) beads treated by different drying methods

Corn starch at room temperature has a granular structure and remains in granular form under the applied conditions. Starch granules were the largest sized particles of the fillers investigated in this

study. Beads composed of alginate with a higher concentration of starch were thus larger in size than beads made from alginate with cellulose powder. It is possible that the granules had a stabilizing effect and to a certain degree prevented the collapse of the internal structure of the beads during drying.

The drying method had a considerable effect on the size and swelling behavior of the beads. As shown in Fig. 2.1b, larger sizes were observed for the freeze-dried samples. During lyophilization enclosed water was quickly removed from the beads without major collapse of the pores which might more or less reflect the state in which they were under wet conditions. All freeze-dried samples showed a highly porous structure as can be seen from their cross-sections (discussed below, Fig. 2.4f). A homogenous filler distribution in alginate and a relatively strong interaction between the polysaccharide components and alginate might have resulted in the less compact, but still mechanically stable bead structure with large pores as observed by SEM.

2.3.2 Swelling ratios

After the beads were prepared via crosslinking in $CaCl_2$ solution they were air- or freeze-dried. Their average moisture loss (freshly made-to-dry) was within the range of 92-95.5% when air-dried and 94-95.5% when freeze-dried, thus the original drying method did only little influence the moisture loss.

The dried beads were then exposed to distilled water and their swelling ratios determined. Fig. 2.2 shows a comparison of swelling ratios of air-dried and freeze-dried beads. Air-dried beads clearly had a more compact structure upon crosslinking than freeze-dried ones. Their average swelling ratios were around 50-65% with alginate-CNC beads showing a somewhat higher water uptake

(approximately 85%) than alginate alone or any of the beads containing the other fillers. Using air drying, CNC obviously assisted the water uptake the most, while xylan admixture affected the swelling of the freeze-dried beads the most. Freeze-dried alginate-xylan beads reached 190%, while alginate-CNC showed an average swelling ratio of 135%. For all other blended beads and alginate alone the difference between freeze drying and air drying was much less pronounced. Especially cellulose powder and starch (columns b and c in Fig. 2.2) seem to have little impact on the water uptake. These beads were obviously comparably compact regardless which drying method was used. The interaction of the beads was further investigated by low-field NMR.

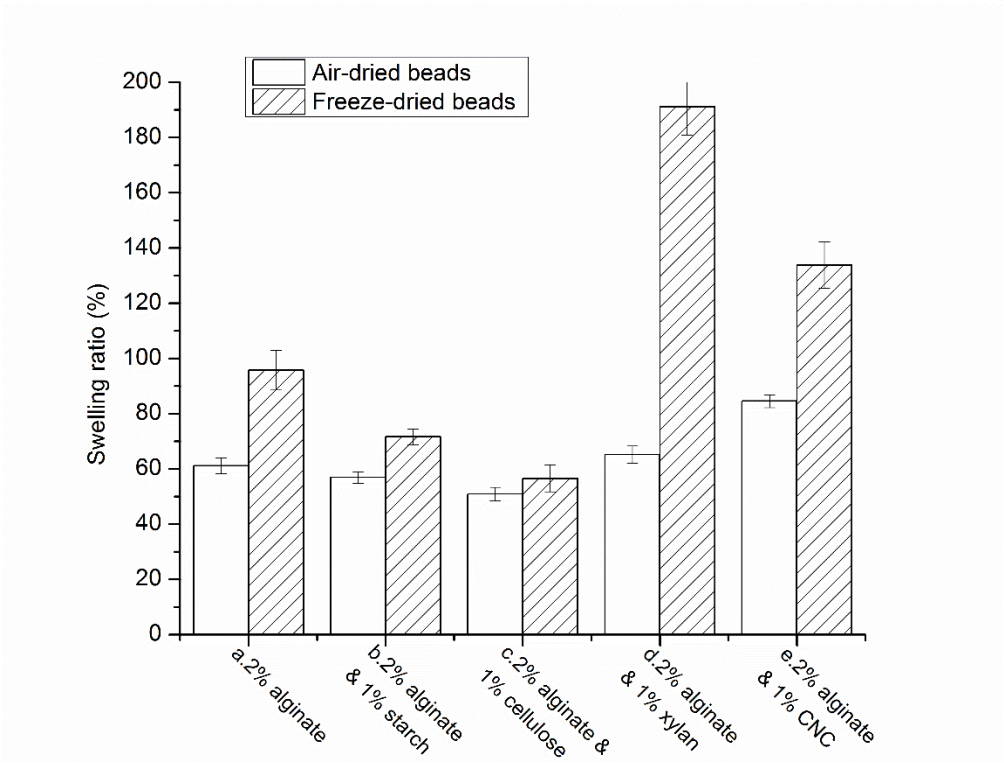

Fig. 2.2 Swelling ratios of air-/freeze-dried beads

2.3.3 Interaction of water with the beads

Relaxation time distributions from low-field NMR indicated that all the samples exhibited three peaks at 20-40 ms (T2(1)), 450-725 ms (T2(2)) and 800-1700 ms (T2(3)) assigned to bound water,

free water and unadsorbed surface water, respectively [20,21]. For the purposes of the current paper, bound water and free water are defined as chemisorbed water on surfaces, and liquid water in pores, respectively. The former, in which water interacts strongly with the surface, accounts for its short relaxation time, while the latter, due to compartmentalization in small openings will have relaxation times shorter than surface water. In related work on alginate films, bimodal distributions of relaxation times were observed, perhaps indicative of bound and free water, but without a surface water peak probably due to differences in sample preparation and structure [20]. Table 2.1 shows relaxation times of beads made with different compositions. In general, the freeze-dried samples had longer relaxation times than air-dried and for T2(1) and T2(2) the results largely parallel each other. The longer relaxation times associated with the freeze-dried samples are indicative of less interaction between the water and the constituents of the beads. The longest relaxation times (T2(3), Table 2.1), assigned to unadsorbed surface water, were very similar for all formulations except for the beads containing xylan, which was much shorter. Given the hydrophilicity of xylan and its solubility in alginate at low concentrations, this might be interpreted in terms of increased interaction between the water and xylan on accessible surfaces of the beads. While relaxation times can give an indication of the interaction between a compound and water, it is difficult to make a clear distinction between these interactions and the porosity or pore sizes/geometries of the sample. Both factors strongly govern the swelling behavior and both will influence relaxation times. T2(1) relaxation times of the different polysaccharide-alginate samples in this study did not show an apparent relationship with the swelling ratio. The reason could be that the amount of water bound to polysaccharide by physico-chemical interaction only played an insignificant role for the total uptake of water in swollen beads.

Table 2.1 Relaxation times related to air-/freeze-dried beads

Beads components	T2(1) (ms)		T2(2) (ms)		T2(3) (ms)	
	Air-dried	Freeze-dried	Air-dried	Freeze-dried	Air-dried	Freeze-dried
2% alginate	23	32	520	542	1420	1570
2% alginate & 1% cellulose powder	25	33	660	700	1675	1680
2% alginate & 1% CNC	23	29	505	600	1670	1600
2% alginate & 1% starch	31	34	620	720	1640	1700
2% alginate & 1% xylan	30	40	600	450	955	830

An effort was made to correlate the observed T2(2) relaxation time of the samples with their swelling capacity in water. As the T2(2) relaxation time associated with free water decreased, the swelling ratio of the beads increased. In the case of air-dried samples, alginate-CNC beads clearly showed the best correlation between the gravimetrically determined swelling ratio and the correspondingly shortest T2(2) values. In regard to the freeze-dried samples, alginate-xylan beads had the shortest T2(2) and the highest swelling ratio.

Beads prepared from alginate with starch or cellulose had comparatively low swelling ratios and longest T2(2). Thus, it could be argued that the value of relaxation time T2(2) mostly showed a positive correlation with swelling ratio of different beads under the same drying method.

Overall, both T2(1) and T2(2) of air-dried samples were shorter than those of freeze-dried samples with the same polysaccharide composition. This indicated that air-dried beads had a stronger interaction with both bound and free water, probably caused by a more compact structure, allowing

more sorbed water locked inside the beads. The more open, porous structure of freeze-dried samples allowed more surface adsorbed water (as observed with T2(3)). The only exception were alginate/xylan beads in regard to T2(2)). Xylan is the only one of the polysaccharides explored in this study that has some solubility in alginate while the other admixed polysaccharides remained as crystalline or granular fillers.

2.3.4 Morphological analysis

Scanning electron microscopy (SEM, Fig. 2.3 and 2.4) was used to show the overall shapes and surface morphologies of the 2% alginate control beads and 2% alginate beads containing one of the following blended-in polysaccharides: 1% starch, 1% cellulose powder, 1% CNC, or 1% xylan. The method of drying did not seem to play a major role for the overall shape of the beads. They all were more or less spherical with a somewhat rough surface appearance. However, as it can be expected, the type of admixture impacted the surface morphology.

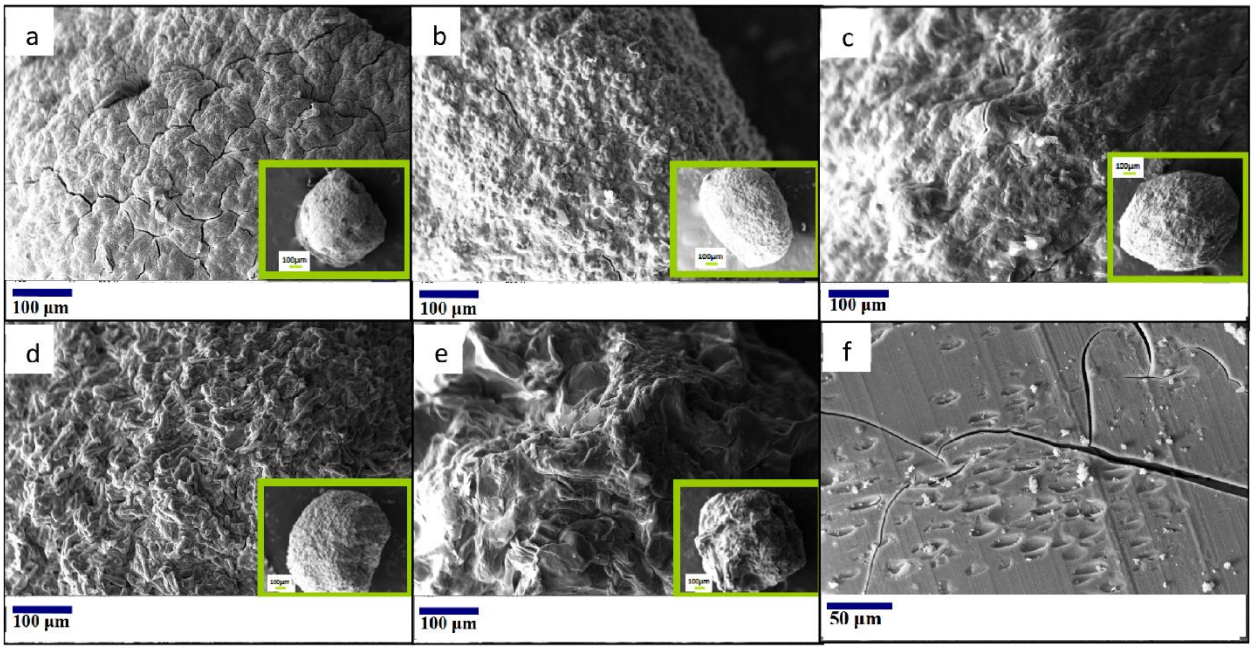

Fig. 2.3 Surface morphologies and bead shapes of different air-dried polysaccharide beads (a)

alginate only, (b) 2% alginate with 1% starch, (c) 2% alginate with 1% xylan, (d) 2% alginate with 1% cellulose powder, (e) 2% alginate with 1% CNC, (f) cross section of an alginate only bead, representative of all other beads

The differences in appearance may be attributed to the physical form of the polysaccharide and the way the polysaccharide combinations were able to interact. The air-dried beads formed from alginate alone had relatively smooth surfaces (Fig. 2.3a), while beads containing 1% starch showed a more granular structure probably because the original granular structure from corn starch was still preserved (Fig. 2.3b). Blending alginate with 1% cellulose powder created a coarser surface morphology of the resulting beads (Fig. 2.3d). The roughest surfaces were observed with xylan and CNC admixtures (Fig. 2.3c and e).

Unexpectedly the cross-sections of the beads did not differ significantly. Fig. 2.3f depicts a cross-section through an alginate bead, representative of all other beads. They all had a fairly compact structure with more or less equal sized pores and some cracks. Freeze dried samples, on the other hand, showed large open structures of interconnected pores (Fig. 2.4f).

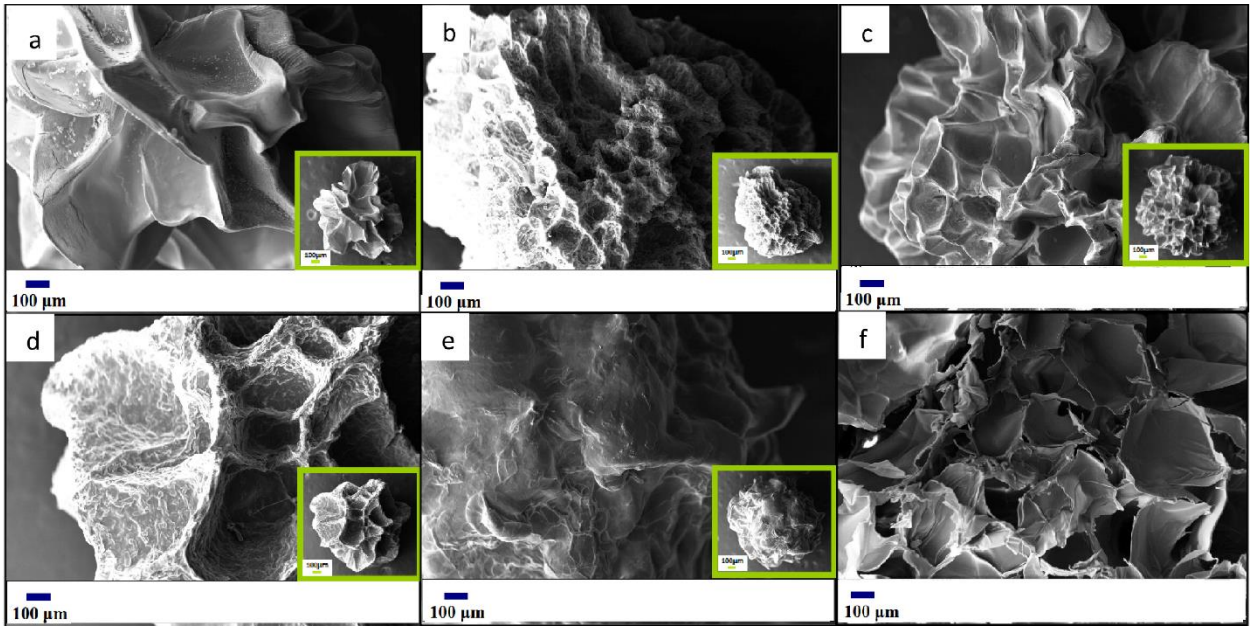

Fig. 2.4 Surface morphologies of different freeze-dried polysaccharide beads (a) alginate alone (b) 2% alginate with 1% starch (c) 2% alginate with 1% xylan (d) 2% alginate with 1% cellulose powder (e) 2% alginate with 1% CNC (f) cross section morphology of alginate bead without additional polysaccharide

Compared to the air-dried beads with the same composition, the SEM images of freeze-dried samples (Fig. 2.4) all showed highly corrugated surfaces with more or less smooth walls (for example, alginate with xylan, Fig. 2.4c, compared with alginate containing cellulose powder, Fig. 2.4d). In alginate beads containing starch, the granular structure of starch could still be detected.

2.3.5 pH-dependent charge density changes in polysaccharide suspensions

The charge densities as a function of the pH value of different polysaccharide mixtures are presented in Fig. 2.5. Alginic acid soldium salt solutions alone and with either starch, CNC, or cellulose powder had an initial pH of 7.4. As mentioned above, these fillers remained in solid form regardless of the pH value. The first point of detectible charge density was at pH 8. Neither cellulose nor starch contain ionizable groups in the neutral and low alkaline range that could contribute to the overall charge density. Granular uncharged fillers might lower detectable charges in the overall solution. Cellulose particles show some swelling at pH values above pH 10 and influence the titration result to a certain extent. Above pH 11 all beads began to disintegrate.

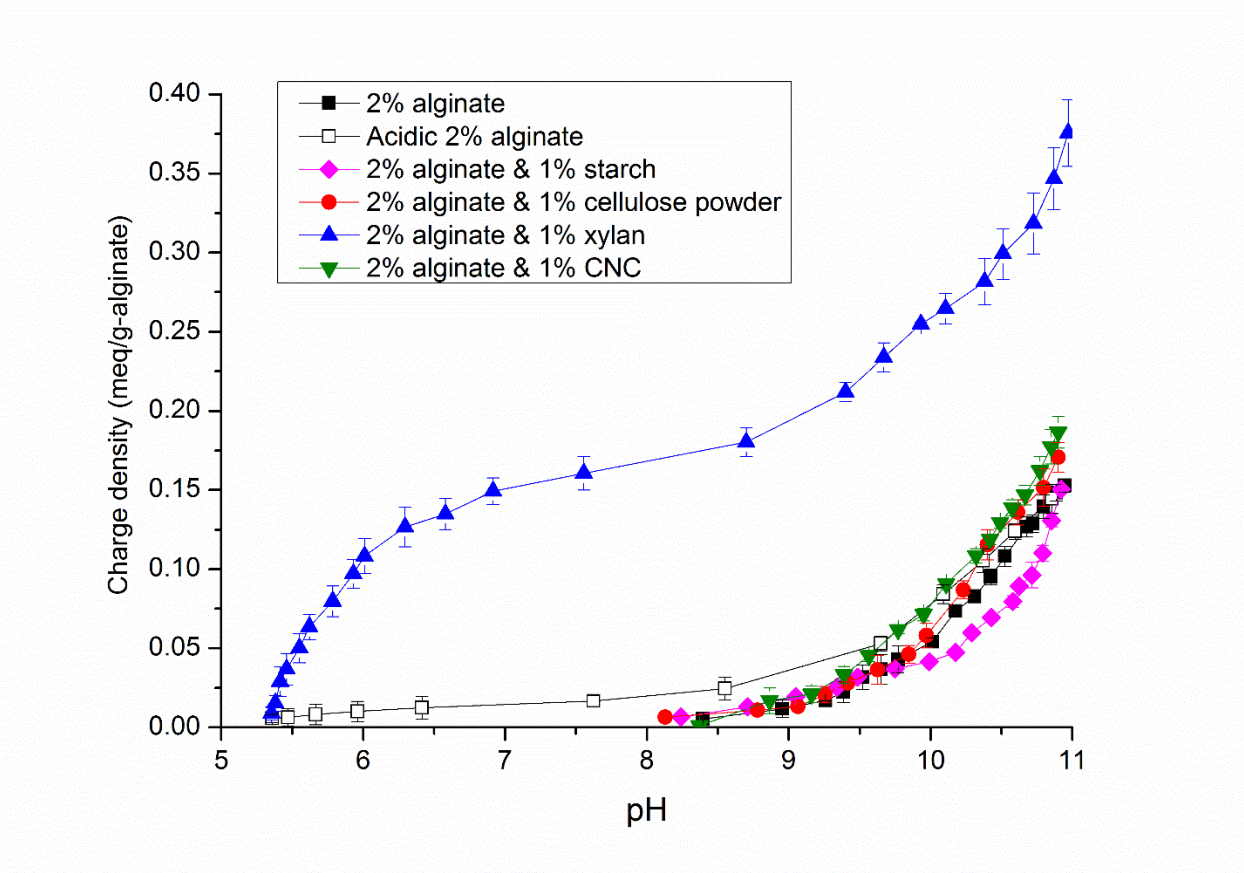

Fig. 2.5 Charge density of blended polysaccharide suspensions with different compositions

The admixture of xylan lowered the initial pH to 5.4. Therefore an alginate control sample of the same pH was prepared (termed "acidic 2% alginate" in Fig. 2.5) that was measured simultaneously with xylan containing alginate. However when using a potentiometric method, it has been mentioned in literature that it is difficult to clearly separate the effect of composition of the polymer and its charge density from other parameters such as water content in a swollen polymer or differing porosity when solid surfaces are involved [18]. Therefore, only the difference between two comparable samples rather than absolute values might give an indication of available charges. In the case of xylan-alginate beads the higher charge density at any given pH value must be attributed to additional carboxylic acid groups from xylan that dissociated at a lower pH together

with additional dissociated carboxylic acid groups of alginate. These results suggest that beads containing xylan could be expected to be most effective in terms of binding cationic compounds (e.g., MB) if formed at a pH close to 11.

2.3.6 Methylene blue sorption

It was assumed that beads prepared with alginate still contain a certain amount of dissociated carboxylic acid groups after crosslinking. These negative charges could then form electrostatic interactions with positively charged groups in MB. Besides negative charges, the porous structure of the beads was expected to enhance the sorption of the dye. Experiments were performed to investigate whether the incorporation of fillers into alginate would have a measurable effect on its cation sorption capabilities. It was assumed that the driving force was both the formation of electrostatic interactions and sorption phenomena. A series of samples of air-dried (Fig. 2.6a) and freeze-dried beads (Fig. 2.6b) prepared with $CaCl_2$ solution at pH 9 were exposed to aqueous MB solutions and the capacity for the dye pick-up measured. Additionally, wet (never-dried) beads prepared in a $CaCl_2$ solution at pH 9 and at higher alkalinity (pH 11) were studied to evaluate the effect of changes in charge density on MB uptake (Fig. 2.7a and b, respectively). As mentioned above, wet beads became unstable above pH 11.

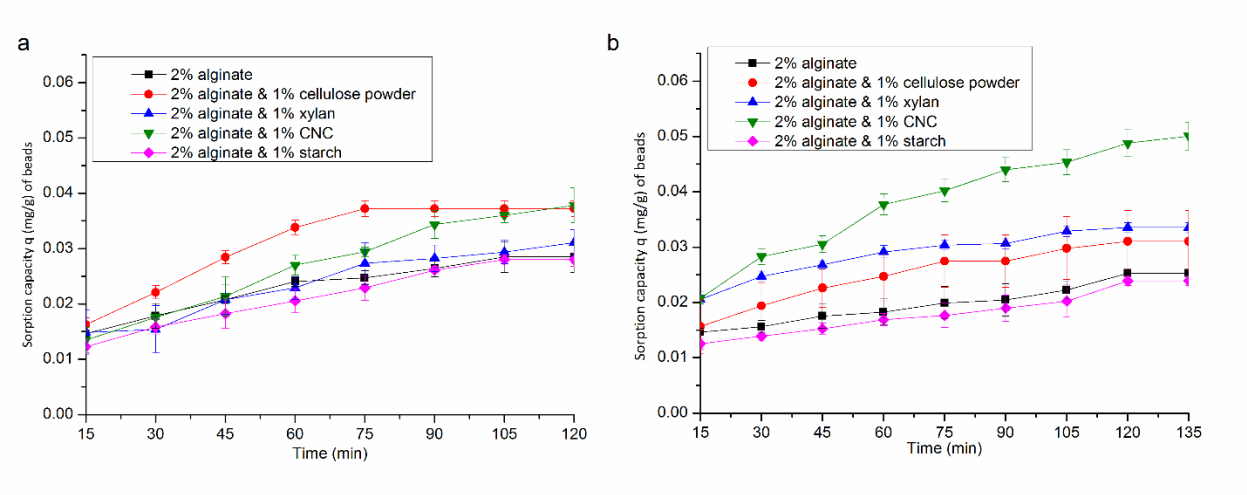

Fig. 2.6 MB sorption capacity of (a) air-dried beads, (b) freeze-dried beads

Fig. 2.6 illustrates that air-drying and freeze-drying of the beads did not lead to major differences in MB sorption of the resulting beads that could be associated with the drying method. Within the air-dried series, beads containing cellulose powder initially showed slightly higher MB sorption than the other samples, while the addition of CNC to alginate had increased MB sorption in the case of freeze-drying. Although very small, the higher sorption of cationic MB could indicate the presence of a few negatively charged sulfate groups left in CNC from its production by acid hydrolysis from cellulose and thus might have been available for MB binding. These groups, however, did not show as a measurable difference in regard to the pH-dependent charge density (Fig. 2.5). The overall lowest MB sorption for all types of beads was observed with starch as the admixture. It is possible that starch acted as a simple filler, reducing the accessible internal surface area for positively charged groups.

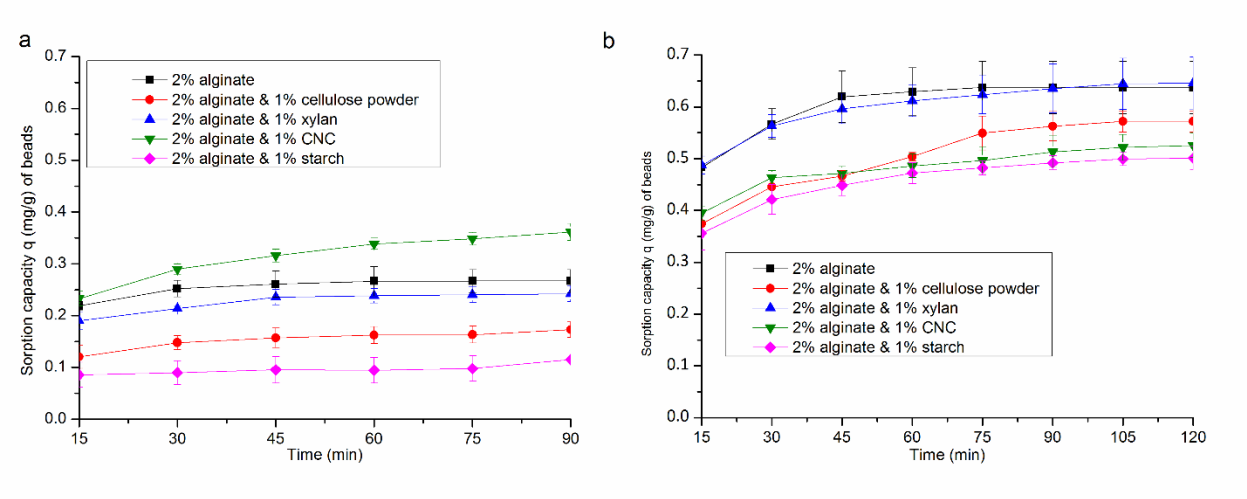

Fig. 2.7 Sorption capacity for MB of wet (never-dried) beads crosslinked at (a) pH 9 and (b) pH 11

It was further observed that freshly made, wet (never-dried) beads had a 5-10 times higher overall MB sorption capacity than dried beads (Fig. 2.7a), which could be due to a higher accessibility of internal surfaces and charged groups within the beads. Upon drying, some pores might have collapsed and possibly remained unavailable during subsequent exposure to aqueous dye solution. As could be expected, in this series CNC-alginate samples again showed the highest MB uptake capacity as it had been the case with freeze-dried samples. Pure alginate and xylan-alginate beads showed very similar sorption behavior and starch-alginate beads were the samples with the lowest sorption capacity for MB.

If the crosslinking pH was changed from 9 to 11 (Fig. 2.7b), MB uptake essentially doubled for all samples. At pH 11, pure alginate and xylan-alginate MB sorption capacity was basically indistinguishable, but clearly higher than in the case of all other samples. CNC and cellulose powder addition did not result in a major difference which matches the results of charge density at this pH (Fig. 2.5). It should however be stressed that for all samples charge density increase cannot

be the only factor responsible for MB sorption but also the morphology and porosity of the beads.

2.3.7 Sorption kinetics studies

The sorption capacities at equilibrium (q_e), rate constants (k_1 or k_2) and correlation coefficients (R^2) were calculated and are listed in Table 2.2. The sorption processes occurred quite rapidly and most of MB could be removed within the initial 75 min for air-dried beads, 90 min for freeze-dried beads, 60 min for wet beads crosslinked at pH 9 and 75 min for wet beads crosslinked at pH 11. Thus, both pseudo-first-order and pseudo-second-order were fitted and adjusted to the data from the initial time period of the experiments.

For pseudo-first-order model, the plot of $\ln(q_e-q_t)$ against t resulted in a straight line with the slope of k_1 and intercept of $\ln q_e$. As can be seen from Table 2.2, the correlation coefficient for the sorption of cationic model MB from different beads ranged from 0.836 to 0.997. The pseudo-second-order rate constant k_2 and the equilibrium sorption capacity q_e can be determined from the slope and intercept of the plot of t/q_t versus t. From Table 2.2, higher correlation coefficients of 0.902 to 1 for different beads were obtained. Therefore, pseudo-second-order kinetics seems to better fit the experiments. Pseudo-second-order is based on the assumption that the rate limiting step is the chemical sorption or chemisorption involving valency forces between sorbent and sorbate [22]. It appears to more suitably represent the sorption of MB by the investigated beads compositions in both dried and wet conditions.

Table 2.2 Kinetic parameters of MB sorption of air-dried, freeze-dried, wet beads crosslinked at pH 9 and pH 11

Beads composition/state		Pseudo-first-order			Pseudo-second-order		
		q_e (mg/g)	k_1 (min^{-1})	R^2	q_e (mg/g)	k_2 (g mg^{-1} min^{-1})	R^2
2% alginate	Air-dried	0.020	0.023	0.977	0.031	1.64	0.988
	Freeze-dried	0.013	0.011	0.982	0.023	3.76	0.992
	Wet (pH 9)	0.443	0.119	0.899	0.286	0.787	1.000
	Wet (pH 11)	0.454	0.068	0.987	0.696	0.224	0.999
2% alginate & 1% cellulose	Air-dried	0.044	0.040	0.947	0.058	0.401	0.972
	Freeze-dried	0.021	0.021	0.968	0.034	1.48	0.993
	Wet (pH 9)	0.082	0.035	0.981	0.183	0.714	0.999
	Wet (pH 11)	0.370	0.033	0.903	0.613	0.143	0.991
2% alginate & 1% xylan	Air-dried	0.028	0.024	0.897	0.036	0.887	0.902
	Freeze-dried	0.017	0.021	0.981	0.035	2.52	0.999
	Wet (pH 9)	0.149	0.065	0.966	0.264	0.614	0.999
	Wet (pH 11)	0.232	0.032	0.988	0.670	0.264	1.000
2% alginate & 1% CNC	Air-dried	0.034	0.018	0.979	0.044	0.551	0.944
	Freeze-dried	0.042	0.020	0.974	0.057	0.560	0.973
	Wet (pH 9)	0.228	0.038	0.995	0.398	0.229	0.999
	Wet (pH 11)	0.155	0.023	0.936	0.527	0.397	0.999
2% alginate & 1% starch	Air-dried	0.021	0.018	0.990	0.029	1.43	0.985
	Freeze-dried	0.014	0.011	0.990	0.021	3.21	0.989
	Wet (pH 9)	0.033	0.009	0.836	0.099	4.15	0.999
	Wet (pH 11)	0.234	0.034	0.997	0.531	0.245	0.999

2.4 Conclusions

A series of polysaccharide beads were prepared from alginate and either one of two types of cellulose (nanocrystalline or powder), starch or xylan and crosslinked with calcium ions. It was

found that different bead sizes, swelling properties and surface morphologies resulted due to the nature and concentration of the admixed polysaccharide. The method of drying (air-drying or lyophilization) also showed a significant effect. As could be expected, freeze-dried beads were more porous and adsorbed more water. However, it was surprising that not all freeze-dried samples also adsorbed more cationic contaminants (as exemplified by methylene blue as a model cation) than air-dried beads. Low-field NMR spectroscopy was used to attempt to differentiate between tightly bound non-freezing water, free water and surface water. The results indicated that air-dried samples had a stronger interaction with water than freeze-dried due to their denser structure. Overall, beads containing xylan showed the highest interaction with water. These beads also had the highest charge density at pH values below 7. In regard to the adsorption of cations, such as the model dye methylene blue, freshly made beads containing xylan adsorbed most if the beads were prepared at a more alkaline pH 11, while when made at a pH of 9, the ones containing nanocrystalline cellulose (CNC) adsorbed slightly more. Thus, for the removal of cationic contaminants from water CNC might be the most effective additive to alginate, while xylan might be preferred if higher water sorption is the goal.

2.5 References

[1]. Vijayaraghavan K, Yun YS (2008) Biosorption of C.I. Reactive Black 5 from aqueous solution using acid-treated biomass of brown seaweed Laminaria sp. Dyes Pigments 76: 726-732

[2]. Gupta VK, Suhas (2009) Application of low-cost adsorbents for dye removal--a review. J. Environ Manage 90: 2313-2342

[3]. Robitzer M, David L, Rochas C, Renzo FD, Quignard F (2008) Nanostructure of calcium alginate aerogels obtained from multistep solvent exchange route. Langmuir 24: 12547-12552

[4]. Zhu H, Srivastava R, Brown JQ, McShane M (2005) Combined physical and chemical immobilization of glucose oxidase in alginate microspheres improves stability of encapsulation and activity. J Bioconjugate Chem 16: 1451-1458

[5]. Ai Q, Yang D, Zhu Y, Jiang Z (2013) Fabrication of boehmite/alginate hybrid beads for efficient enzyme immobilization. Ind Eng Chem Res 52: 14898-14905

[6]. Torres E, Mata YN, Blazquez ML, Munoz JA, Gonzalez F, Ballester A (2005) Gold and Silver Uptake and Nanoprecipitation on Calcium Alginate Beads. Langmuir 21: 7951-7958

[7]. Kacar Y, Arpa C, Tan S, Denizli A, Genc O, Anca MY (2002) Biosorption of Hg (II) and Cd (II) from aqueous solutions: comparison of biosorptive capacity of alginate and immobilized live and heat inactivated Phanerochaete chrysosporium. Process Biochem 37: 601-610

[8]. Anca MY, Arpa C, Ergene A, Bayramoglu G, Genc O (2003) Ca-alginate as a support for Pb (II) and Zn (II) biosorption with immobilized Phanerochaete chrysosporium. Carbohyd Polym 52: 167-174

[9]. Bayramoglu G, Denizli A, Bektas S, Arica MY (2002) Entrapment of Lentinus sajor-caju into Ca-alginate gel beads for removal of Cd (II) ions from aqueous solution: preparation and biosorption kinetics analysis. Microchem J 72: 63-76

[10]. Aravindhan R, Fathima NN, Rao JR, Nair BU (2007) Equilibrium and thermodynamic studies on the removal of basic black dye using calcium alginate beads. Colloid Surface A 299: 232-238

[11]. Gotoh T, Matsushima K, Kikuchi KI (2004) Preparation of alginate-chitosan hybrid gel beads and adsorption of divalent metal ions. Chemosphere 55: 135-140

[12]. Lu L, Zhao M, Wang Y (2007) Immobilization of Laccase by Alginate–Chitosan Microcapsules and its Use in Dye Decolorization. World J Microbiol Biotechnol 23: 159-166

[13]. Rocher V, Siaugue JM, Cabuil V, Bee A (2008) Removal of organic dyes by magnetic alginate beads. Water Res 42: 1290-1298

[14]. Rocher V, Bee A, Siaugue JM, Cabuil V (2010) Dye removal from aqueous solution by magnetic alginate beads crosslinked with epichlorohydrin. J Hazard Mater 178: 434-439

[15]. Liu L, Wan Y, Xie Y, Zhai R, Zhang B, Liu J (2012) The removal of dye from aqueous solution using alginate-halloysite nanotube beads. J Chem Eng J 187: 210-216

[16]. Li M, Tshabalala MA, Buschle-Diller G (2016) Formulation and characterization of polysaccharide beads for controlled release of plant growth regulators. J Mater Sci 51: 4609-4617

[17]. Provencher SW (1982) CONTIN: A general purpose constrained regularization program for inverting noisy linear algebraic and integral equations. Comput Phys Commun 27: 229-242

[18]. Boyer TH, Singer PC (2008) Stoichiometry of removal of natural organic matter by ion exchange. Environ Sci Technol 42: 608-613

[19]. Qiu H, Lv L, Pan B, Zhang Q, Zhang W, Zhang Q (2009) Critical review in adsorption kinetic models, J Zhejiang Univ Sci A 10: 716-724

[20]. Fabich HT, Vogt SJ, Sherick ML, Seymour JD, Brown JR, Franklin MJ, Codd SL (2012) Microbial and algal alginate gelation characterized by magnetic resonance. J Biotechnol 161: 320-327

[21]. Elder T, Houtman C (2013) Time-domain NMR study of the drying of hemicellulose extracted aspen. Holzforschung 67: 405-411

[22]. Elzatahry, AA., Soliman, EA., Mohy Eldin, MS, Elsayed Youssef, M. (2010) Experimental and simulation study on removal of methylene blue dye from alginate micro-beads, J Am Sci 6: 846-851

Chapter 3 Formulation and characterization of polysaccharide beads for controlled release of plant growth regulators

3.1 Introduction

Agrochemicals, such as pesticides, herbicides, fertilizers and plant hormones, improve the production of crops and play an important role in maintaining the increasing demand of food for a growing global population. While conventional agrochemical formulations are using a greater amount of chemicals over a longer period of time than is actually needed, the harmful effect of these chemicals of causing crop damage, environmental pollution and health risks is the real major limitation of their application [1-3]. Evaluating and balancing beneficial and adverse effects of agrochemicals can be problematic [4]. Hence, safe handling of these chemicals is essential and appropriate application systems, aiming at lower dosage and site-specific release at a slower and more controlled rate over a prolonged period of time, must be found [5,6]. Controlled release systems can optimize the applicable efficiency of bioactive chemicals, and minimize the residues of agrochemicals [2]; thus a feasible approach to reduce efficiency loss, pollution and health risks due to leaching, volatilization and biodegradation needs to be developed.

In recent years, a great deal of interest has been focused on exploring low cost, biodegradable and non-toxic materials as reservoirs/carriers for improved controlled discharge of agrochemicals[7,8]. Polysaccharides are among the most promising candidates of all renewable compounds for this purpose [6,9,10] and play an important role, especially in the form of hydrogels [2,11-15] and beads [16-24]. They are capable of slowly releasing agrochemicals and simultaneously increasing the water-holding capacity of soil [25]. In addition, polysaccharides can also serve as nutrients in

the field after degradation by soil microorganisms. Alginic acid is an anionic naturally abundant polysaccharide extracted from brown seaweed and soil bacteria. Chemically, it is a linear copolymer composed of two monomers, (1-4)-linked β-D-mannuronic acid (M) and α-L-glucuronic acid (G) residues of different ratios and distribution along the chains [26]. In aqueous solution at neutral pH, alginate contains a significant amount of negative charges due to deprotonated carboxylic acid groups. These negative charges enable alginate to induce repulsive electrostatic forces and to swell as well as to interact with positively charged ionic groups. Alginate exhibits a sol-gel transition by forming the so-called "egg-box" structure when sodium counter-ions are substituted with divalent cations, such as calcium, zinc, or barium [26].

Beads made from crosslinked sodium alginate have been found to be suitable as a supporting matrix for controlled release of agrochemicals as documented in numerous publications. For instance, pesticide/herbicide/plant growth regulator loaded sodium alginate beads were crosslinked with glutaraldehyde [20] and various divalent metal ions, e.g. calcium [18, 19, 21-23] and nickel [18]. Various clays such as kaolin have been used as additives in polysaccharide based controlled release systems to further reduce the release rate [21, 22]. It was found that the composition of the beads and the type of crosslinking agent (cation type and concentration), as well as other factors, such as crosslinking time, surface coating, and pH of the release media also affected the release kinetics.

Moreover, neutral and anionic polysaccharide fillers such as starch, cellulose and xylan have potential to improve the alginate bead system by influencing the release rate of the targeted agrochemicals. However, to our knowledge a comparative study of different combinations of polysaccharide and kaolin fillers in combination with a surface coating has not yet been performed.

The work described in this paper is concerned with polysaccharide-kaolin blended beads without/with polyethylenimine surface coating. The beads before coating are composed of alginate, kaolin and an additional polysaccharide as the filler (starch, cellulose powder, cellulose nanocrystals (CNC) and xylan). Both the bead components and the cationic coating were designed to influence the internal and external properties of beads and to optimize the controlled release of phenylacetic acid (PAA). The average size and size distribution of dry beads, their swelling ratios, mechanical strength under compression and their morphologies were studied. In addition, the cumulative release of PAA, an anionic plant growth regulator, was assessed. The application of the cationic polyelectrolyte polyethylenimine (PEI) after the beads were crosslinked with calcium ions, was intended to reduce the release rate of PAA by forming an extra electrostatic barrier to the free passage of PAA. It was found that the cumulative release was clearly affected by the composition of the beads and the PEI coating. The admixture of the polysaccharide filler proved to be a key factor affecting morphology, while the PEI coating influenced the swelling ratio, compressive strength and cumulative release of PAA.

3.2 Experimental

3.2.1 Materials

Alginic acid sodium salt (medium viscosity), cellulose (powder, ~20 micron), xylan from beech wood and polyethylenimine (branched, PEI) were purchased from Sigma Aldrich. Cellulose nanocrystals (CNC) were provided by the U.S. Department of Agriculture, Forest Products Laboratory, Madison, WI. Phenylacetic acid (PAA) was purchased from Alfa Aesar and kaolin was from Ward's Science. Corn starch was food grade, and calcium chloride was from Merck. All materials were used as received.

3.2.2 Preparation of beads

Various combinations of aqueous suspensions carrying 0.03 M PAA were prepared by mixing 2% w/v sodium alginate, 2% kaolin w/v with 1% w/v corn starch, cellulose powder, xylan or CNC, respectively, with deionized water. All suspensions were mixed homogenously using a magnetic stirrer at 1000 rpm at room temperature for 3 h. The suspensions were added dropwise to 0.2 M aqueous calcium chloride solution as the crosslinking agent through a 10 mL syringe with a needle size of 18G×$1^1/_2$. The syringe was pushed by a syringe pump at a constant rate of 4 mL/min. The beads were left in calcium chloride solution to harden for 30 min with gentle stirring. Finally, they were washed three times with deionized water to remove the calcium chloride left on the surface. A portion of freshly made beads were air dried for 48 h; a second batch was further crosslinked with 2% and a third batch with 4% w/v PEI aqueous solution for 2 h. The beads were washed with deionized water and air dried for 48 h.

3.2.3 Size measurement of beads

Optical microscopy was used to measure the size of air-dried beads. 20 beads within each sample and three diameters for each bead (maximum, minimum and diagonal) were measured and the average diameter was calculated and recorded.

3.2.4 Swelling ratios of beads

The weight of the dried beads and beads immersed in deionized water for 48 h at room temperature were determined. The swelling ratio was evaluated using Equation 1.

$$\text{Swelling ratio } \% = \frac{W_s - W_d}{W_d} \times 100\% \qquad \text{(Equation 3.1)}$$

where W_s is the weight of the water-swollen beads, and W_d the weight of the dried beads.

3.2.5 Mechanical strength measurements

10 beads of each composition were compressed individually by an Instron® 5565 Tensile Testing machine, with the compressive force increasing from 0 to 10 kg at a rate of 10 kg·min^{-1}. The compressive force and deformation of each bead were recorded. After the test, the force that caused 30% bead deformation was averaged and plotted in relationship to the bead composition.

3.2.6 Scanning electron microscopic (SEM) and energy dispersive spectroscopy (EDS) analysis of beads

The surface morphology of dried beads before and after the compression test as well as morphology of bead cross sections before compression were observed by scanning electron microscopy (SEM) at a 20 kV accelerating voltage and working distance 5.5-9 mm, using a Zeiss EVO 50 Variable Pressure SEM. The samples were sputter-coated with gold in an EMS 550X Auto Sputter Coating Device.

Weight percentage of calcium and other elements on the beads' surface and at the interior cross-sections were measured by energy dispersive spectroscopy (Inca EDS system) connected with SEM at a 20kV accelerating voltage and working distance 9 mm. The samples were sputter-coated with carbon in an EMS 550X Auto Sputter Coating Device.

3.2.7 Cumulative release of PAA into water

One g of beads was placed into a beaker with 100 mL deionized water, and stirred at 100 rpm for 48 h. Three mL of solution was measured by UV-Vis spectroscopy every 30 min during the first

4 h, then at 5, 6, 24 and 48 h. After each measurement, three mL of fresh deionized water was added to the beaker to keep the volume of the solution constant at 100 mL. The measurement procedure for one sample was repeated three times. The cumulative release (%) was calculated according to Equation 3.2.

$$\text{Cumulative release } (\%) = 100\% \times (C_i V + C_{i-1} R + C_{i-2} R + \cdots + C_{i-n} R)/W \quad \text{(Equation 3.2)}$$

where i is the number of measurement, C_i is the concentration of PAA in the solution at i-th measurement, V is the total volume of release solution, R is the volume of fresh medium and W is the total weight of PAA entrapped in the beads before the release.

3.2.8 Release kinetics

Many controlled release products are designed on the principle of embedding the chemical in a porous matrix. When liquid penetrates the matrix and dissolves the drug, then the chemical diffuses into the exterior liquid. Higuchi was the first to derive an equation to show the release of a chemical from an insoluble matrix as the square root of a time-dependent process simplified as follows:

$$Q_t = k_H (t)^{0.5} \quad \text{(Equation 3.3)}$$

Q_t is the amount of chemical released (cumulative % release) in time t and k_H is the release rate constant for the Higuchi model.

3.3 Results and Discussion

3.3.1 Size and size distribution analysis

Average diameter and standard deviation of beads dried at room temperature were plotted and the results are displayed in Fig. 3.1. Beads crosslinked only in 0.2 M $CaCl_2$ solution are marked as "series 1"; those coated with 2% PEI and 4% PEI are designated "series 2" and "series 3", respectively. Beads composed of 2 % alginate and 2% kaolin constituted the control sample. All other beads contained 1% of an additional polysaccharide filler based on the control sample.

Beads made of different components within the same series showed small differences in average diameter. The concentration of alginate and the polysaccharide filler was always kept at a ratio of 2:1 (w/w). The size of the filler polysaccharide and the interaction of filler molecules with the alginate bead (e.g. repulsion between different functional groups, crosslink density) may have influenced the actual observed size of the beads. For instance, beads containing xylan showed the second largest size among all samples without PEI coating. This may be attributed to the additional negatively charged carboxylic acid group allowing more Ca^{2+} to combine within the alginate bead. Thus it is likely that beads containing xylan formed a stronger electrostatic interaction to support the bead structure during drying.

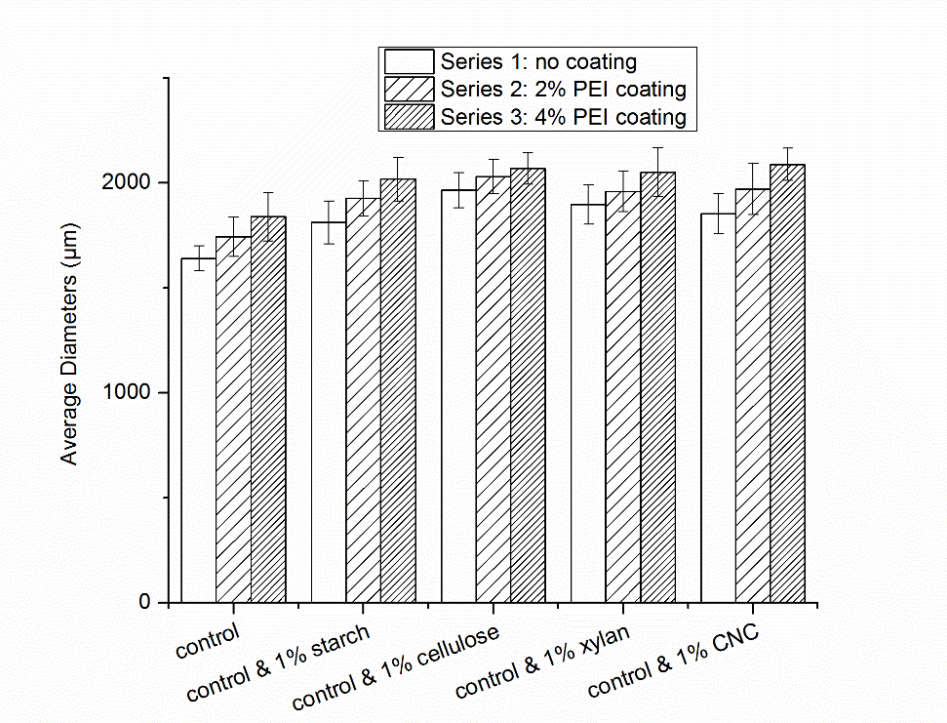

Fig. 3.1 Average diameters of beads; series 1: beads with no coating, series 2: beads with 2% PEI coating, and series 3, beads with 4% PEI coating

Table 3.1. Beads' weight increase (%) after coating with 2%/4% PEI (aq)

	2% PEI	4% PEI
Control	3.9±0.08	15.1±0.61
Control & 1% starch	4.1±0.11	16.3±0.43
Control & 1% cellulose	3.6±0.18	14.8±0.37
Control & 1% xylan	5.4±0.32	21.8±0.64
Control & 1% CNC	5.1±0.27	19.6±0.86

Since the PEI was branched and had a high molecular weight (M_n~10,000) it was not expected to penetrate the beads' surface structure but only form a coating on the exterior of the beads. This assumption was confirmed scanning electron microscopy.

As can be seen from Fig. 3.1 and Table 3.1, beads of comparable composition were slightly larger (3-5%) when coated with 2% PEI aqueous solution. At 4% PEI concentration, the bead' sizes increased by 6-11% compared to the uncoated samples. In contrast to the bead size, the weight increase of the beads after coating was much larger than the size increase especially with 4% PEI (aq). This may indicate that PEI as a positive-charged polyelectrolyte created additional electrostatic interactions with additional negative charges from COO^- and may exchange Ca^{2+} from the previous Ca^{2+}-COO^- crosslink sites, resulting in beads with a firmer and denser structure at the outside layer. It was observed that the higher the concentration of PEI, the firmer and denser the bead surface. It can be hypothesized that the weight increase mostly contributed to the increase of surface layer density.

3.3.2 Swelling ratios

Table 3.2 shows the swelling ratios of beads without coating as well as with 2 and 4% PEI coating. Beads without coating had rather similar swelling ratios. However, beads with PEI coating clearly showed higher swelling ratios. Even though it has been argued that beads with PEI coating are surrounded by a firmer surface layer, the layer itself may still contain highly branched PEI and thus be able to absorb liquids. Therefore, this may be the major factor contributing to the observed greater swelling ratio. Overall, beads containing xylan and CNC and coated with 2% and 4% PEI solution showed the highest swelling, especially in the case of xylan. This may be the result of additional negative charges on xylan interacting with more amino groups on PEI. In chapter 2, charge density of different polysaccharide combinations, alginate with xylan clearly had the highest negative charge density among all samples.

Table 3.2. Swelling ratios data (%) of beads without/with coating

	No coating	2% PEI coating	4% PEI
Control	24.5±0.87	34.1±1.19	61.4±1.02
Control & 1% starch	26.7±0.42	39.3±0.81	78.1±1.09
Control & 1% cellulose	22.2±0.59	32.1±0.78	62.3±1.28
Control & 1% xylan	31.1±0.82	46.8±0.73	96.2±1.16
Control & 1% CNC	27.9±0.53	41.7±0.62	84.4±1.91

3.3.3 Mechanical strength analysis

Mechanical properties of three series of beads along with beads made of alginate alone were investigated. Beads made of alginate alone were compared with those reinforced with kaolin to investigate the effectiveness of kaolin in improving the mechanical strength of the alginate beads. The average compressive force causing 30% deformation of each bead sample is shown in Fig. 3.2. Beads made from alginate alone proved to be the weakest. Beads within each series showed a slight difference, which likely indicated that the polysaccharide filler did not sufficiently enhance the mechanical strength of the bead. However, PEI coating indeed strengthened the bead structure and higher PEI coating resulted in higher mechanical strength overall. To be more specific, beads without coating reached 30% deformation by a force of 2.5-4 kg. For beads coated in 4% PEI solution, the compressive force increased to 6-8.5 kg. Some cracks appeared at the edges of the beads when the compressive force reached the maximum set in the experiment (10 kg) as could be demonstrated by SEM (see below, Fig. 3.6)

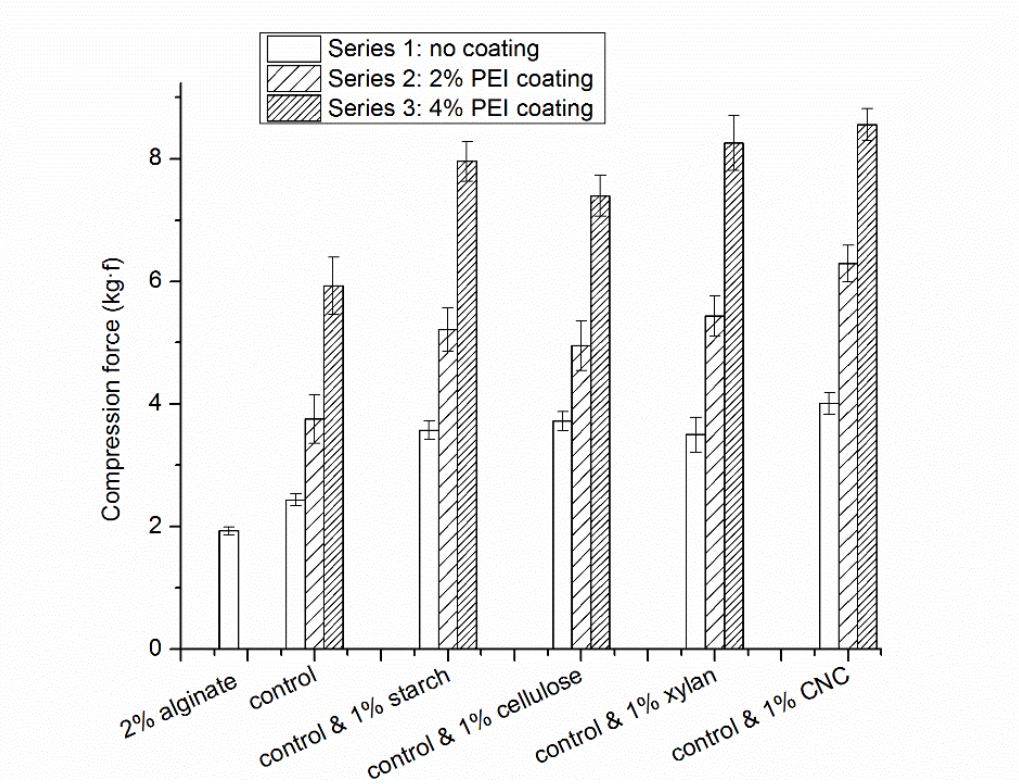

Fig. 3.2 Compression force applied to 30% deformation of beads

3.3.4 Morphology analysis and elemental composition

The surface morphologies of different beads without coating are shown in Fig. 3.3. The differences in appearance may be attributed to the physical form of the polysaccharide filler and the way the polysaccharide combinations were able to interact. The beads formed from alginate and kaolin alone had relatively smooth surfaces (Fig. 3.3a), while beads containing 1% starch showed a more granular structure probably because the original granular structure from corn starch was still preserved (Fig. 3.3b). Blending alginate with 1% cellulose powder created a coarser surface morphology of the resulting beads (Fig. 3.3c). The roughest surfaces were observed with CNC admixtures (Fig. 3.3e).

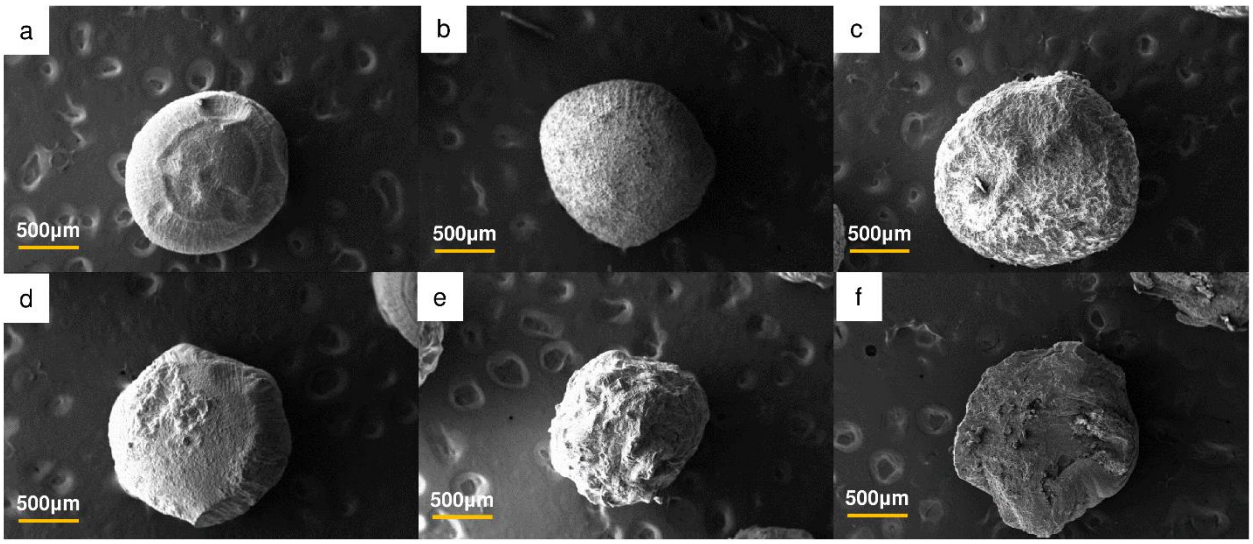

Fig. 3.3 Surface morphology of beads composed of (a) control, (b) control & 1% starch, (c) control & 1% cellulose, (d) control & 1% xylan, (e) control & 1% CNC, (f) cross section of control sample

The cross-sections of the beads did not differ significantly. Fig. 3.3f depicts a cross-section through a control bead, representative of all other beads. They all had a fairly compact structure with more or less equal sized pores and some cracks.

As can be seen in Figs. 3.4a and c, beads with xylan, as representative of all samples, adopted a rougher surface after coating in PEI solution. The more coating was applied, the more rugged the surface tended to become. It can also be seen from Figs. 3.4b and d, the cross sections of cut beads with PEI coating were only rough on the outside the bead, not in the interior.

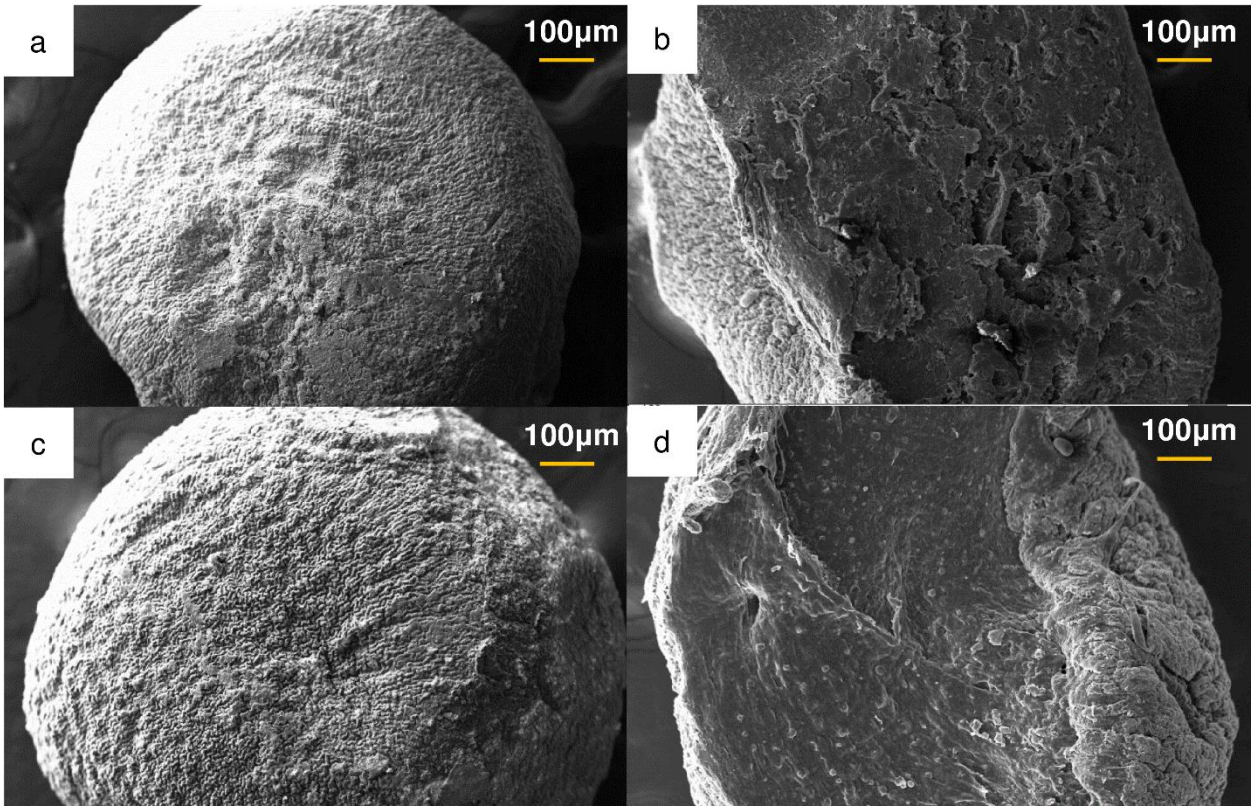

Fig. 3.4 Bead surface and cross section morphologies: control with 1% xylan: 2% PEI, 4% PEI coating (a) and (c); (b) cross section of (a), (d) cross section of (c)

EDS in conjunction with SEM was used to determine the element composition of the surface of the beads in comparison to the interior at cross sections. Representative of all samples, data for beads with CNC with/without PEI coating are presented in Table 3.3 and Fig. 3.5. Generally, Ca and Cl were directly from crosslinking. A small amount of Na indicated that a minor portion of sodium alginate could not bind with calcium ions. Sulfur probably originated from sulfate groups on CNC which had been hydrolyzed by sulphuric acid, and Al, Si, and Ti came from kaolin. Carbon and oxygen are not reported as they exist in all samples and are distributed evenly within each sample.

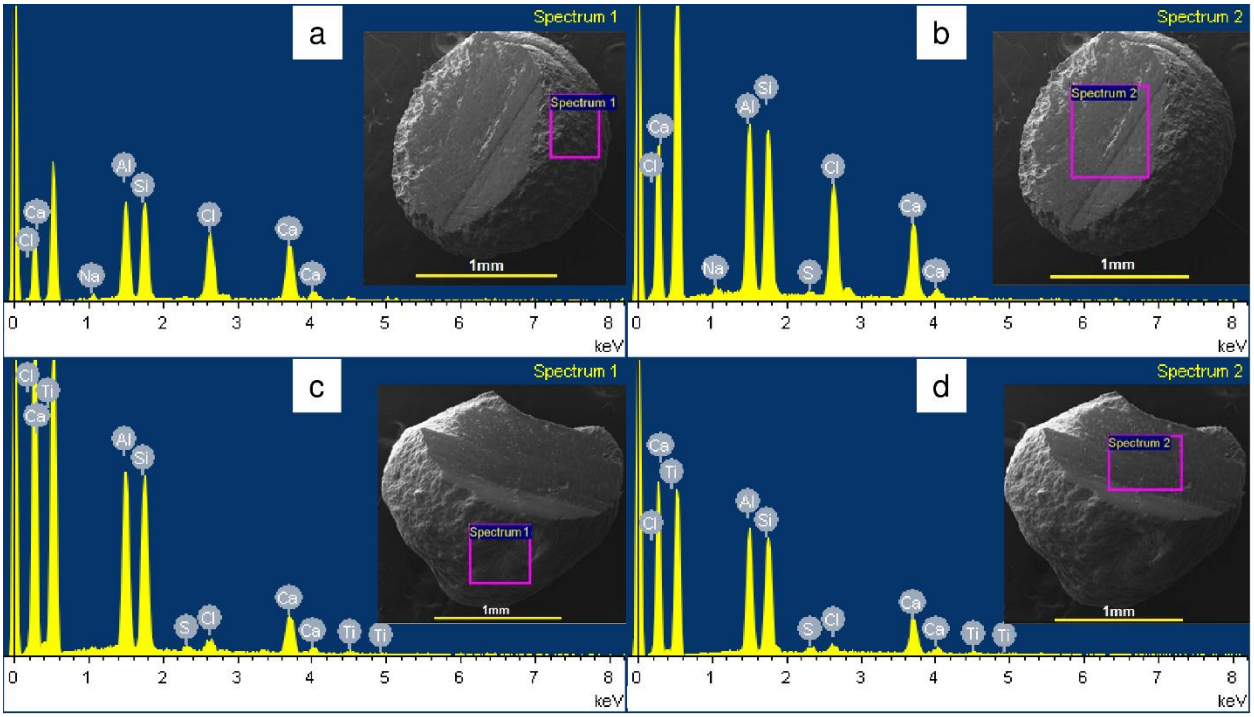

Fig. 3.5 SEM-EDS of beads (control containing 1% CNC) without coating: (a) surface, (b) interior; with 2% PEI coating: (c) surface, (d) interior

Table 3.3. Elements found on the surface and the interior of beads (control containing 1% CNC) without and with 2% PEI coating (%wt).

	No coating		2% PEI	
Elements	Surface	Interior	Surface	Interior
Na	1.30	1.29	---	---
Al	19.56	20.94	29.45	28.51
Si	27.28	28.11	45.63	42.72
S	---	1.13	1.90	2.57
Cl	24.93	26.35	4.68	3.58

Ca	26.93	22.17	16.63	20.63
Ti	---	---	1.70	1.99

As can be seen from Table 3.3, Figs. 3.5a and b, beads without coating had a higher weight percentage of calcium on the surface compared to the central cross-section. This might be due to the relatively short crosslinking time of 30 min and Ca^{2+} could not sufficiently reach all carboxylic groups in the center area of beads.

After coating in PEI solution, the content of calcium on the exterior of the beads was lower than that of the central cross-sectional area (Table 3.3, Figs. 3.5c and d; shown for 2% PEI). Overall the concentration of PEI did not play a major role as coating in 2 and 4% solution yielded very similar results. Most likely the positively charged imine groups of PEI successfully competed with and exchanged a portion of Ca^{2+} on the surface of beads by forming stronger electrostatic interactions with carboxylic groups. An additional factor was that PEI molecules were not able to penetrate the bead's interior, and thus, PEI coating could only affect the amount of Ca^{2+} found on the beads' surface. Simultaneously the weight percentage of Cl decreased upon coating. This could be attributed to Cl^- becoming dispersed in PEI solution during the coating process.

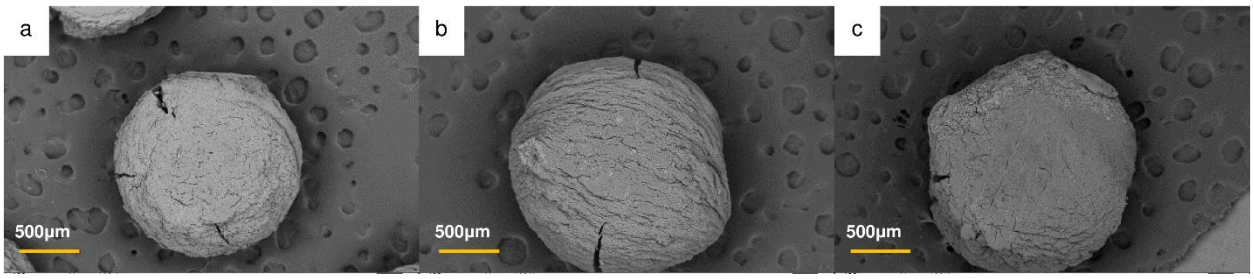

Fig. 3.6 Beads (control & 1% CNC) surface morphology after compression by 10kg force, (a) no coating, (b) 2% PEI coating, (c) 4% PEI coating

The surface morphology of a single bead changed somewhat after compression under an increasing force of 0 to 10 kg (Fig. 3.6). The beads were not completely crushed after withstanding 10 kg force (98.1 N), instead, they flattened, and cracks appeared at the edges. However, with more PEI coating on the surface, the beads tended to have less cracks.

3.3.5 Cumulative release analysis

The effects of the polysaccharide filler and the PEI solution concentration used for the coating were investigated in light of their controlled release capabilities. Figs. 3.7 and 3.8 show the time release of PAA from beads of different compositions without or with further coating at different concentrations of PEI solutions. The time release of PAA was determined for a total of 48 h of release at fixed time intervals.

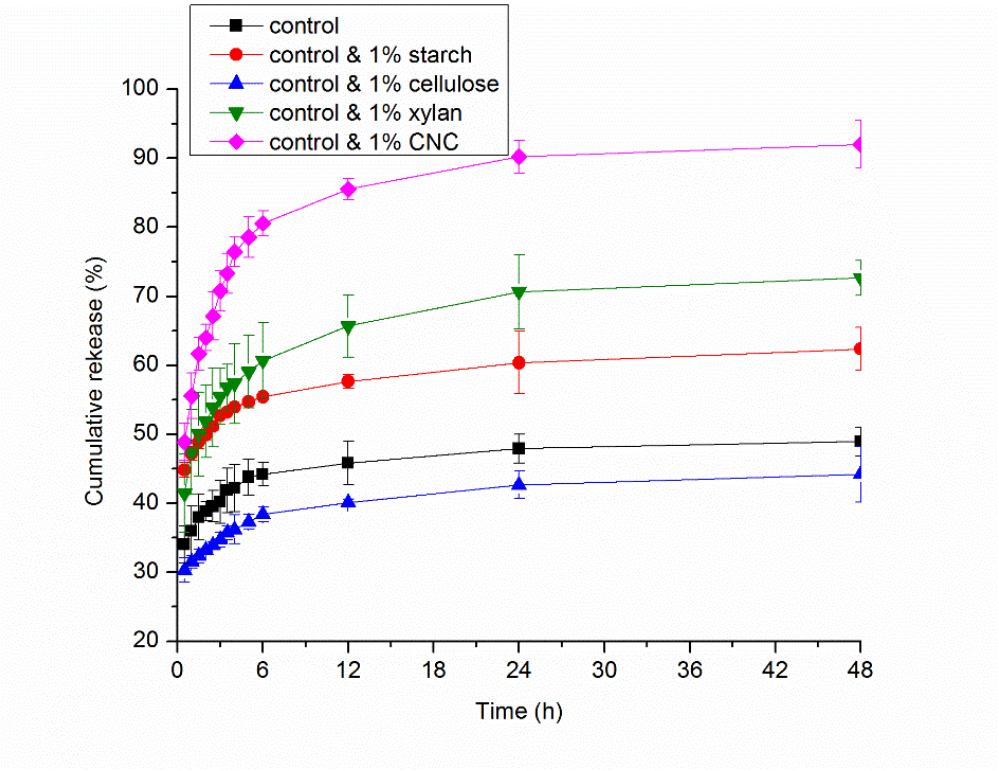

Fig. 3.7 Cumulative release of beads with no coating

As can be seen from Fig. 3.7, there is an initial fast release (30% to 50%) of PAA from the beads within the first 30 min regardless of the filler added to the control sample. This release may mainly be attributed to PAA molecules located at the open structure close to the bead surface when in contact with water. The cumulative release decreased after 6 h and remained stable after 24 h. At the end of 48 h, a portion of PAA was still trapped inside the beads probably due to the interaction with positive charges. The presence of CNC, xylan or starch as fillers increased the PAA release rate compared with the control sample. This may indicate that these three polysaccharides either created a more open structure with alginate and kaolin or hindered the sites from forming electrostatic interactions with Ca^{2+} in the beads. It is also possible that the additional negatively charged carboxylic acid groups contributed by xylan may have formed stronger electrostatic interactions with Ca^{2+} and thus repelled some of the PAA during the crosslinking and release procedures. Similarly, the enhanced release of PAA by the xylan-containing beads could also result from repulsion of the PAA by the negatively-charged carboxyl groups on the xylan. Thus, the release of PAA within the first 48 h could potentially be regulated by carefully designed polysaccharide combinations.

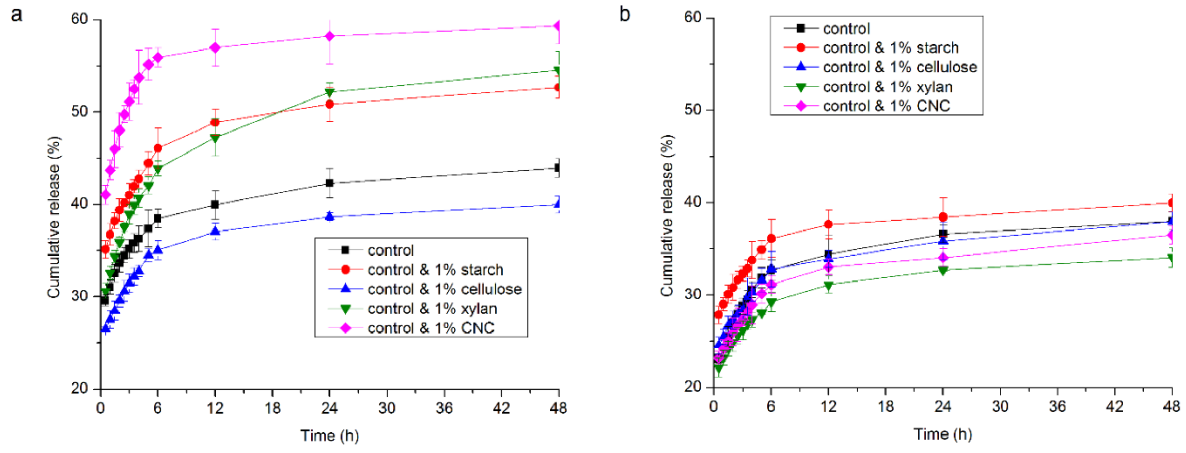

Fig. 3.8 Cumulative release of beads with (a) 2% PEI coating, (b) 4% PEI coating

When the beads were coated with PEI, the surface layer acted as a barrier to the free passage of PAA during the initial 30 min to 48 h by forming a denser structure. Further, the outside layer may have extra positive charges originating from PEI which may hinder PAA from being readily released from the beads. From Figs. 8a and b, it can be seen that the cumulative release from beads composed of xylan and CNC decreased the most compared with all other samples. This could be interpreted as an indication that beads with xylan and CNC contained more PEI in their surface layer as discussed in the previous section.

3.3.9 Release kinetics

Table 3.4 Release kinetic parameters of PAA from beads

Beads composition		Higuchi model	
		k_H	R^2
Control	uncoated	5.97	0.987
	2% PEI	5.08	0.995
	4% PEI	5.80	0.996
Control & 1% starch	uncoated	6.23	0.976
	2% PEI	6.18	0.997
	4% PEI	4.74	0.996
Control & 1% cellulose	uncoated	4.71	0.995
	2% PEI	5.22	0.993
	4% PEI	4.80	0.985
Control & 1% xylan	uncoated	10.5	0.963

	2% PEI	7.75	0.996
	4% PEI	4.05	0.999
Control & 1% CNC	uncoated	18.6	0.982
	2% PEI	8.99	0.986
	4% PEI	4.69	0.994

The release rate constant k_H of Higuchi model is related to several factors, including the diffusion coefficient, solubility of chemical in dissolution media, porosity (the fraction of matrix that exists as pores or channels into which the surrounding liquid can penetrate), tortuosity (the path length of diffusion caused by branching and bending of the pores) and chemical content per cm^3 of matrix. Overall, this model matches PAA release from beads due to their morphologies. In addition, the correlation coefficients of PAA release from uncoated and coated beads were between 0.963 and 0.999 which again shows the Higuchi model matches well for the mechanism of PAA controlled release from these beads.

3.4 Conclusion

In this research, a series of alginate and kaolin based beads were formed with added polysaccharide fillers, crosslinked in $CaCl_2$ solution and further coated in 2% or 4% w/v PEI solution. Beads with PEI coating were slightly larger than beads without coating. PEI coating supported swelling of the surface layer due to its branched structure and affected the surface morphology of the beads. The cumulative release of a plant growth regulator, phenylacetic acid, clearly depended on the composition of the beads. The larger release rates of the beads that contained polysaccharide fillers indicated that the beads possessed a more open structure with hindered electrostatic interaction

and larger repulsive force allowing more PAA to be released. The faster cumulative release by some polysaccharide combinations would be preferable when shorter release times are required. The PEI coating caused slowing of the release of PAA by forming a denser and positively charged surface layer. A steady release rate was reached before 48 h, and it is hypothesized that the release could be prolonged to longer time periods by careful selection of bead composition.

3.5 References

[1]. McCrink-Goode M (2014) Pollution: A global threat, Environ Int 68:162-170.

[2]. Bajpai AK, Giri A (2003) Water sorption behavior of highly swelling (carboxymethylcellulose-g-polyacrylamide) hydrogels and release of potassium nitrate as agrochemical, Carbohydr Polym 53:271-279.

[3]. Abhilash PC, Singh N (2009) Pesticide use and application: an Indian scenario, J Hazard Mater 165:1-12.

[4]. Hayo MG, van der Werf (1996) Assessing the impact of pesticides on the environment, Agriculture, Ecosystems & Environment 60(2–3):81–96.

[5]. Arias-Estévez M, López-Periago E, Martínez-Carballo E, Simal-Gándara J, Mejuto JC, Garcia-Rio L (2008) The mobility and degradation of pesticides in soils and the pollution of groundwater resources, Agriculture, Ecosystems & Environment, 123(4):247–260.

[6]. Bai C, Zhang S, Huang L, Wang H, Wang W, Ye Q (2015) Starch-based hydrogel loading with carbendazim for controlled-release and water absorption, Carbohydr Polym 125:376-383.

[7]. Roy A, Singh SK, Bajpai J, Bajpai AK (2014) Controlled pesticides release from biodegradable polymers, Cent Eur J Chem, 12:453-469.

[8]. Kumar S, Chauhan N, Gopal M, Kumar R, Dilbaghi N (2015) Development and evaluation of

alginate–chitosan nanocapsules for controlled release of acetamiprid, Int J Biol Macromol 81:631-637.

[9]. Campos EVR., Oliveira JZ de, Fraceto LF, Singh B (2015) Polysaccharides as safer release systems for agrochemicals, Agron Sustain Dev 35:47-66.

[10]. Kashyap PL, Xiang X, Heiden P (2015) Chitosan nanoparticle based delivery systems for sustainable agriculture, Int J Biol Macromol 77:36-51.

[11]. Aouada FA, de Moura MR, Orts WJ, Mattoso LHC (2010) Polyacrylamide and methylcellulose hydrogel as delivery vehicle for the controlled release of paraquat pesticide, J Mater Sci 45:4977–4985.

[12]. Bortolin A, Aouada FA, de Moura MR, Ribeiro C, Longo E, Mattoso LHC (2012) Application of polysaccharide hydrogels in adsorption and controlled-extended release of fertilizers processes, J Appl Polym Sci 123:2291–2298.

[13]. Jamnongkan T, Kaewpirom S (2010) Potassium release kinetics and water retention of controlled-release fertilizers based on chitosan hydrogels, J Polym Environ 18:413–421.

[14]. Ferreira Almeida P, Almeida AJ (2004) Cross-linked alginate-gelatine beads: a new matrix for controlled release of pindolol, J Control Release 97:431–439.

[15]. Zhong K, Lin ZT, Zheng XL, Jiang GB, Fang YS (2013) Starch derivative-based superabsorbent with integration of water-retaining and controlled release fertilizers, Carbohydr Polym 92:1367–1376.

[16]. Quinones JP, García YC, Curiel H, Covas CP (2010) Microspheres of chitosan for controlled delivery of brassinosteroids with biological activity as agrochemicals, Carbohydr Polym 80: 915–921.

[17]. Sopena F, Cabrera A, Maqueda C, Morillo E (2005) Controlled release of the herbicide

norflurazon into water from ethylcellulose formulations, J Agric Food Chem 53:3540–3547.

[18]. Isiklan N (2007) Controlled release study of carbaryl insecticide from calcium alginate and nickel alginate hydrogel beads, J Appl Polym Sci 105:718–725.

[19]. Kenawy NR, Sakran MA (1996) Controlled release formulations of agrochemicals from calcium alginate, Ind Eng Chem Res 35:3726-3729.

[20]. Kulkarni AR, Soppimath KS, Aminabhavi TM, Dave AM, Mehta MH (2000) Glutaraldehyde crosslinked sodium alginate beads containing liquid pesticide for soil application, J Control Release 63:97–105.

[21]. Singh B, Sharma DK, Kumar R, Gupta A (2010) Controlled release of thiram from neem-alginate-clay based delivery systems to manage environmental and health hazards, Appl Clay Sci 47:384–391.

[22]. Pepperman AB, Kuan JCW (1995) Controlled release formulations of alachlor based on calcium alginate, J Control Release 34:17–23.

[23]. Cho AR, Chun YG, Kim BK, Park DJ (2014) Preparation of alginate-$CaCl_2$ microspheres as resveratrol carriers, J Mater Sci 49:4612-4619.

[24]. Peretz S, Anghel DF, Vasilescu E, Florea-Spiroiu M, Stoian C, Zgherea G (2015) Synthesis, characterization and adsorption properties of alginate porous beads, Polym Bull 72:3169-3182.

[25]. Guilherme MR, Aouada FA, Fajardo AR, Martins AF, Paulino AT, Davi MFT, Rubira AF, Muniz EC (2015) Superabsorbent hydrogels based on polysaccharides for application in agriculture as soil conditioner and nutrient carrier: A review, Eur Polym J 72:365-385.

[26]. Paques JP, van der Linden E, van Rijn CJM, Sagis LMC (2014) Preparation methods of alginate nanoparticles, Adv Colloid Interfac 209:163-171.

Chapter 4 Pectin-blended anionic polysaccharide films for cationic contaminant sorption from water

4.1 Introduction

Wastewater discharged from industrial, agricultural, medical and domestic activities is a major contributor to water pollution worldwide. Heavy metals, dyes, pesticides, and fertilizers are among the most persistent hazardous contaminants [1, 2]. In recent years, pharmaceuticals and personal care product residues have also been detected in water bodies throughout the world [3]. Chemicals, such as cationic antiseptics commonly used in many types of antimicrobial soaps, mouthwashes and toothpastes, pose risks to humans and the aquatic ecosystem, especially when they are accumulated in higher concentrations. [4, 5] Various techniques are being used to remove contaminants from aqueous waste [6]. Among them, adsorption has shown to be one of the most efficient and promising techniques for water purification. [7] However, many sorption methods tend to be expensive to operate and may produce toxic byproducts or residuals. For example, activated carbon has been applied as an effective adsorbent as it has a large surface area, low density as well as chemical stability [8]. However, the high costs of manufacturing and regeneration make its use for large scale wastewater treatment uneconomical [9].

Over the past decades, a variety of biodegradable natural polymers generated interest as sorption matrices due to their non-toxicity, ease of processing, cost-effectiveness and affordability across the world [10]. Polysaccharides are a category of natural materials, derived from abundant, low-cost plant sources. Pectin is an anionic polysaccharide rich in galacturonic acid. In nature, 80% of carboxyl groups of galaturonic acid are esterified with methanol [11]. However, this proportion

can be lower to a varying degree depending on the pectin extraction method used. Divalent ions, e.g. Ca^{2+}, Zn^{2+} can react with free carboxyl groups along the pectin chains and form water-insoluble crosslinks in form of the so-called "egg-box" structure causing rapid gelation [12]. Alginate, another naturally abundant anionic polysaccharide widely distributed in the cell wall of brown algae, is a linear copolymer composed of (1-4)-linked β-D-mannuronic acid (M) and α-L-guluronic acid (G) residues at different ratios and distribution along the chains [13] and is rich in carboxyl groups. The carboxyl groups in monoguluronic sequences of sufficient length enable alginate to also form an "egg-box" structure with various divalent ions. Other anionic polysaccharides follow different ion-sensitive gelation mechanisms; for instance, carrageenan which contains varying amounts of sulfate groups depending on its variety (kappa, iota or lambda carrageenan). Carrageenan can form thermoreversible associated helical structures with mono- but also divalent cations upon gelation [14]. Xanthan, a microbial anionic polysaccharide, is affected by mono- to trivalent cations in its coil-to-helical arrangement due to electrostatic repulsion [15]. Crosslinked polysaccharides have been explored for applications as controlled release carriers of active compounds as well as for effective sorbents. In our previous work, polyethylenimine coated polysaccharide beads were used to successfully control the release of an anionic plant hormone due to heightened positive-negative electrostatic interactions [16]. Several crosslinked polysaccharide matrices have been investigated in different forms of sorption systems in recent years; especially beads were applied to remove heavy metal ions (e.g. gold, silver, mercury, copper, lead, etc.) from effluent [17-23]. Besides heavy metals, dyes are also a severe problem in waste water treatment, since colorants do not easily degrade. Some research approaches have been documented to remove typical dyes with the help of polysaccharide beads [24-29].

To our knowledge, no research has been performed on zinc crosslinked films made from anionic

polysaccharide mixtures for the purpose of removing cationic pollutants. This research is thus aimed at the development of films for water remediation based on natural anionic polysaccharides and their blends with pectin. Properties of films with different composition as well as the effect of poly(4-styrenesulfonic acid-co-maleic acid) sodium salt (PSSMA) as a coating were compared. PSSMA is a negatively charged polyelectrolyte which, pH dependent, contains both weakly and strongly ionized groups. PSSMA has shown potential in nanofiltration membranes and as coating of nanoparticles for removal of contaminants [30, 31]. Two typical cationic dyes, methylene blue (MB) and crystal violet (CV), commonly used in both industrial and medical applications, served as model compounds. Cetylpyridinium chloride (CPC) and benzethonium chloride (BtCl) are antiseptics widely applied in mouthwashes and antibacterial products. The removal of these four cationic model compounds was the focus of this study and films with different composition without/with PSSMA coating were compared in their effectiveness.

4.2 Experimental

4.2.1 Materials

Pectin from citrus peel (galacturonic acid, ≥74.0%), alginic acid sodium salt from brown algae (medium viscosity, M/G ratio of 1.56), xylan from beechwood, carrageenan (predominantly κ carrageenan), xanthan, methylene blue (MB), crystal violet (CV), and poly(4-styrenesulfonic acid-co-maleic acid) sodium salt (PSSMA, M_w~20000, SS:MA 3:1) were purchased from Sigma Aldrich. Zinc acetate dehydrate and benzethonium chloride (BtCl) were obtained from Alfa Aesar. Glycerol was from J. T. Baker. Cetylpyridinium chloride (CPC) was from Acros Organics. All materials were used as received.

4.2.2 Preparation of films

Five homogenous aqueous solutions were prepared by mixing 2% w/v pectin as control film, 1% w/v pectin with alginate, carrageenan, xylan or xanthan (each at a concentration of 1%) with stirring at 60℃. 1% w/v glycerol was added as plasticizer to all solutions aimed to increase the flexibility of the films. 25 mL solutions were transferred into petri dishes (diameter 8.5 cm) and air-dried for 24 h at room temperature. Dried films were immersed in 0.1 M zinc acetate solution as crosslinking agent. All films were allowed to crosslink for 10 min. Finally, they were rinsed with distilled water three times to remove any additional zinc acetate from the surface. A portion of films were dried at room temperature for 24 h; a second batch was further immersed in 1% w/v poly(4-styrenesulfonic acid-co-maleic acid) sodium salt (PSSMA) solution for 10 min. These films were also washed with deionized water and dried at room temperature for 24 h.

4.2.3 Film thickness

A digital micrometer (Testing machines, Inc. Model 49-71, precision ±1 μm) was used to measure the thickness of films with different compositions as well as with/without PSSMA coating. Three films of each composition and five random spots of each film were measured and the averaged values were recorded.

4.2.4 Swelling ratios of films

The exact weight of dried films was determined and the films immersed in deionized water at room temperature. After 10 min, the swollen sample was removed, wiped with tissue paper in order to eliminate excess unabsorbed water and weighed. Measurements were made in triplicate. The swelling ratio was calculated based on Equation 1.

$$\text{Swelling ratio } \% = \frac{W_s - W_d}{W_d} \times 100\% \qquad \text{(Equation 4.1)}$$

where W_s is the weight of the water-swollen films, and W_d the weight of the dried films.

4.2.5 Mechanical properties of films

Films were cut into strips with a width of 12.5 mm and length of 65 mm. To standardize the experimental procedure, samples were stored in a humidity and temperature controlled condition for 24 h at 23 ℃ and 50% R.H. Tensile strength and elongation at break of the films were measured by an Instron® 5565 Tensile Testing machine, using a 100 N load cell, gauge length of 25 mm and crosshead speed of 10 mm/min, respectively. Tensile strength was calculated by dividing the maximum force for film rupture by the cross-sectional area, and elongation at break was calculated as the percentage increase of sample length. Average values of tensile strength and elongation at break were obtained from three strips of each film, three films of each composition.

4.2.6 Scanning electron microscopic (SEM) and energy dispersive spectroscopy (EDS) analysis of films

The surface morphology of films was observed by scanning electron microscopy (SEM) at a 20 kV accelerating voltage and working distance of 5.5-6.5 mm, using a Zeiss EVO 50 Variable Pressure SEM. The samples were sputter-coated with gold in an EMS 550X Auto Sputter Coating Device.

Weight percentages of zinc and other elements on the films' surface were measured by energy dispersive spectroscopy (Inca EDS system) connected with the SEM at a 20 kV accelerating voltage and working distance 9 mm. The samples were sputter-coated with carbon in an EMS

550X Auto Sputter Coating Device.

4.2.7 Sorption capabilities of films and kinetic study of methylene blue (MB), crystal violet (CV), cetylpyridinium chloride (CPC) and benzethonium chloride (BtCl) sorption from aqueous solution

The sorption percentage (%) of two cationic dyes and two antiseptics, MB, CV, CPC and BtCl were investigated with films of different composition without and with anionic polyelectrolyte-PSSMA coating. Films of equal weight were added to 60 mL aqueous MB/CV solution of an initial concentration of 5 mg L^{-1} and CPC/BtCl solution of an initial concentration of 150 mg L^{-1}, respectively. CV and MB solutions were kept at a pH of 7.0; CPC and BtCl solutions at pH 6.2. In order to determine unknown concentrations of MB/CV and CPC/BtCl solutions, a calibration curve was created by UV-Vis measurements from a standard MB/CV/CPC/BtCl solution series with known concentrations at their maximum absorbance wavelength of 665, 590, 260 and 280 nm, respectively. Readings were taken at intervals of 15 min until equilibrium was reached. The formula used to calculate the sorption percentage is given in Equation 2. Three batches of each sample were measured until equilibrium was reached and the average values were plotted.

$$\text{Sorption percentage (\%)} = \frac{C_0 - C}{C_0} \times 100\% \qquad \text{(Equation 4.2)}$$

$$\text{Sorption Capacity } q = \frac{(C_0 - C) \times V}{m} \qquad \text{(Equation 4.3)}$$

C_0 is the initial cationic compound concentration in mg L^{-1}; C is the concentration at intervals of 15 min (mg L^{-1}), V is the volume of sorbent solution (mL) and m is the weight of films (g).

4.2.8 Sorption kinetics

Several mathematical theories in modeling the sorption kinetics of pollutants are available; among them, pseudo-first-order and pseudo-second order kinetics are the most important and commonly used ones. [32] The sorption kinetics of the four cationic compounds can be described by pseudo-first-order (Eq. 4) or pseudo-second-order (Eq.5). To determine which model better reflects the sorption behavior of the films, the experimental sorption capacity and the parameters of all four cationic compounds were fitted to both kinetic models.

Pseudo-first-order kinetic model

$$\log (q_e - q_t) = \log q_e - \frac{k_1}{2.303} t \qquad \text{(Equation 4.4)}$$

q_e and q_t are the amounts of cationic compounds sorbed (mg g^{-1}) at equilibrium and at time t (min), k_1 is pseudo-first-order rate constant (min^{-1})

Pseudo-second-order kinetic model

$$\frac{t}{q_t} = \frac{1}{k_2 q_e^{\,2}} + \frac{t}{q_e} \qquad \text{(Equation 4.5)}$$

q_e and q_t are the amounts of cationic compounds sorbed (mg g^{-1}) at equilibrium and at time t (min), k_2 (g mg^{-1} min^{-1}) is the rate constant of pseudo-second-order.

4.3 Results and discussion

4.3.1 Film formation and average film thickness

Films were formed from pectin solution and crosslinked with zinc acetate in the presence of an additional polysaccharide for a relatively short time period and with addition of a plasticizer. The experimental conditions were chosen to obtain films of sufficient mechanical strength and targeted

at pectin gelation. The intention was to preserve some negative charges along the polysaccharide chain as binding sites for cationic pollutants. Formed films were then coated with a thin layer of polyelectrolyte (PSSMA) to augment the available negative surface charges.

The average thickness of different dried films without and with PSSMA coating are shown in Fig. 4.1. Compared to the thickness of the pectin control film, all films differed somewhat in average thickness. It was interesting that all samples with PSSMA coating were slightly thinner than the respective films without coating. Since PSSMA has a high molecular weight (M_w~20,000), it was not expected to penetrate the film's surface but only to form a dense and tight layer on its exterior. The films had already been crosslinked by forming electrostatic interactions between zinc cations and anionic groups originating from polysaccharides. However, they had not been dried before coating, thus some of the polysaccharide chains were incorporated in the surface coating (see EDS results below). The coating on the film most likely was formed by interaction between the anionic groups from PSSMA and available positive charges from a limited amount of zinc on the film surface after crosslinking. The competition between anionic groups from PSSMA and polysaccharide controlled the formation of the coating to some degree. The slight decrease in thickness observed for all films could possibly be a sign of a thin, but rather dense outside layer.

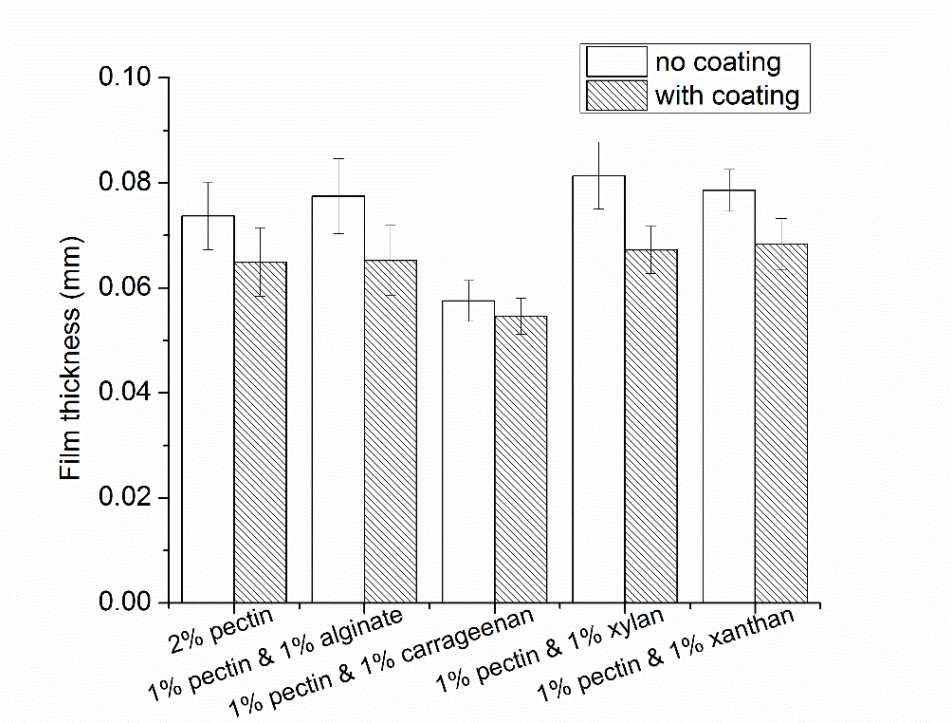

Fig. 4.1 Average thickness of films with different composition without/with PSSMA coating

4.3.2 Swelling ratios

Dried films were immersed in water for 10 min before weighing for water absorption. It was found that for longer immersion than 10 min, water contact time had little influence on the swelling ratio. Fig. 4.2 shows a comparison of swelling ratios of films with different composition without/with PSSMA coating. Uncoated films had swelling ratios of 220 to 550% and with admixed alginate reached the highest swelling which might be explained by its largely uncrosslinked structure under the applied experimental conditions.

Coated films overall had a higher water uptake than uncoated ones. It can be hypothesized that the anionic polyelectrolyte PSSMA coating caused some weakening of the original crosslinking interaction between zinc ions and the polysaccharide at the film interface by strong swelling. PSSMA is a pH dependent polyelectrolyte (see Fig. 4.2). At a pH lower than 5, only -COOH and

-COONa are dissociated, while at pH>5 also -SO_3Na and -SO_3H become available for ionic interaction [Song]. Pectin is stable at neutral pH, but dissolves at alkaline conditions; thus swelling ratios were determined at pH 7 and sorption experiments at pH 6.2-7.

Alginate films again showed the highest swelling ratio (Fig. 4.3). Alginate is the only polysaccharide in this series besides pectin that can effectively crosslink with zinc ions. However, the concentration of zinc ions or the crosslink time may not have been sufficient under the set experimental conditions, leaving alginate largely uncrosslinked and able to considerably swell in water. More negatively charged groups are present that repel each other and expand the space inside the network to hold more water. The coating on the film which seems dense in dry state, did not prevent the swelling of the hydrophilic interior of the films interior underneath. The second highest swelling ratio was observed with xanthan (more than 600%), while other coated films had only moderately swelling ratios in the range of 300-420% on the average.

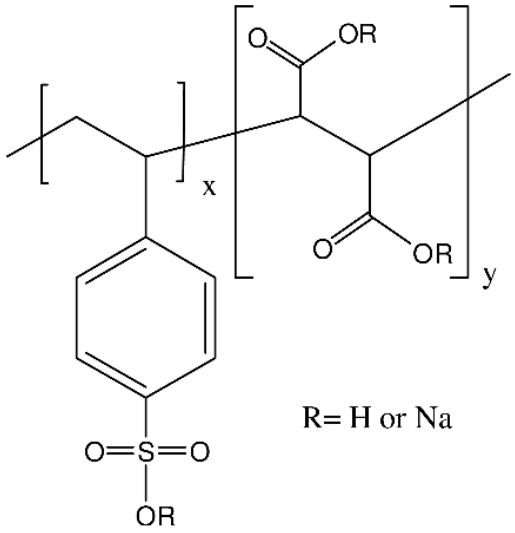

Fig. 4.2 Chemical structure of PSSMA

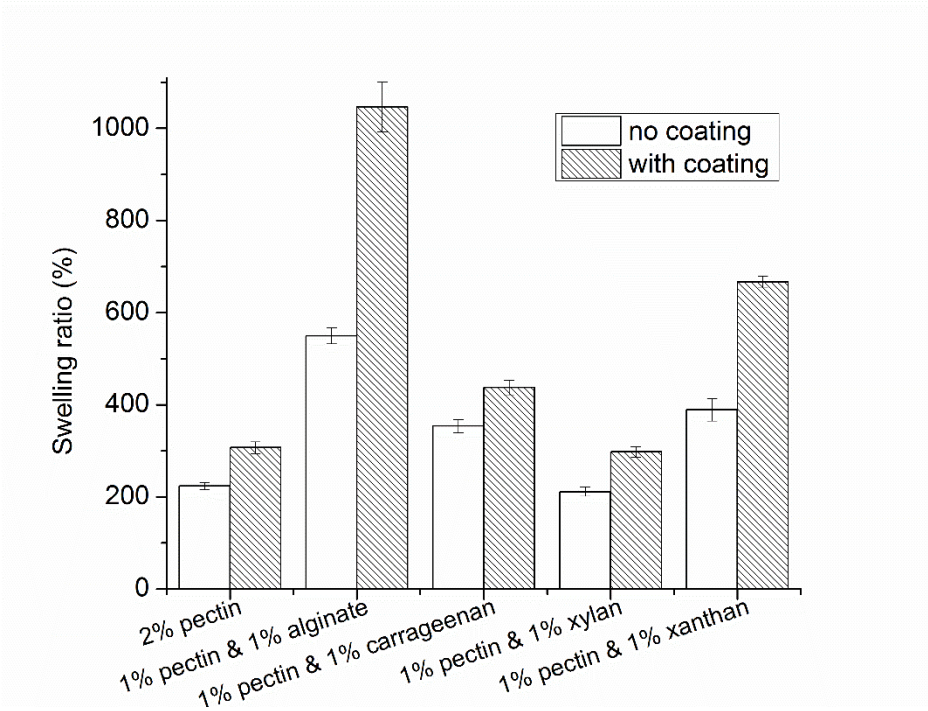

Fig. 4.3 Swelling ratios of films without/with PSSMA coating

4.3.3 Morphology and element composition analysis

Scanning electron microscopy (SEM, Figs. 4.4 and 4.5) was used to illustrate the surface morphology of films composed of 2% pectin control film in comparison to 1% pectin and admixed 1% additional anionic polysaccharides: 1% alginate, 1% carrageenan, 1% xylan, or 1% xanthan before (Fig. 4.4) and after (Fig. 4.5) coating with PSSMA.

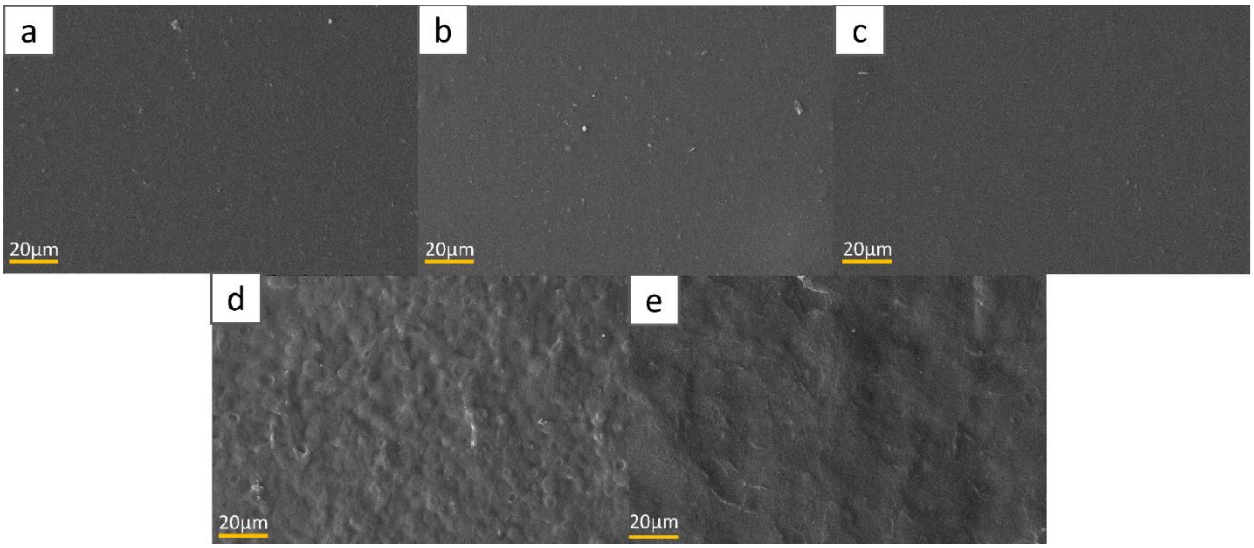

Fig. 4.4 Surface morphologies of uncoated films composed of (a) 2% pectin only, (b) 1% pectin with 1% alginate, (c) 1% pectin with 1% carrageenan, (d) 1% pectin with 1% xylan, (e) 1% alginate with 1% xanthan

It can be seen that pectin control film and films containing alginate or carrageenan had a comparatively smooth surface with little distinguishing features. Xylan and xanthan containing films seemed to have a slightly rougher surface which might have been created during cooling and drying possibly causing some aggregation under the set conditions. After coating with PSSMA, smoother surfaces were observed for all films (Fig. 4.5).

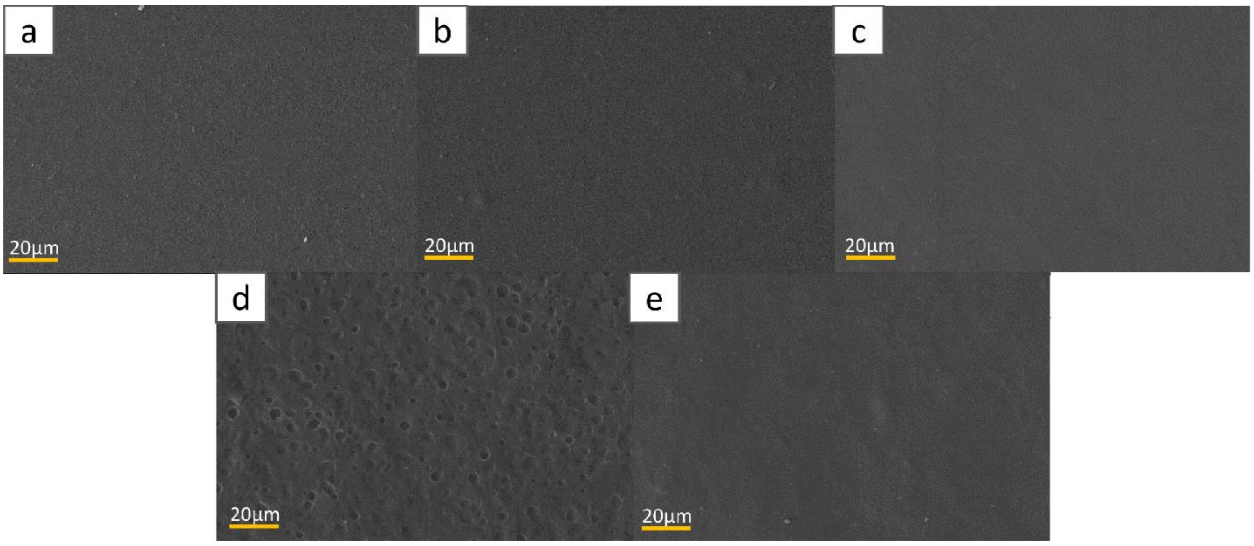

Fig. 4.5 Surface morphologies of PSSMA-coated films composed of (a) 2% pectin only, (b) 1% pectin with 1% alginate, (c) 1% pectin with 1% carrageenan, (d) 1% pectin with 1% xylan, (e) 1% alginate with 1% xanthan

EDS in conjunction with SEM was used to determine the element composition of the film surfaces before and after coating with PSSMA. The results are presented in Table 4.1 (without coating) and Table 4.2 (with coating). Minute impurities in the surface of the films are not reported.

Table 4.1 Elemental analysis of the surface of uncoated films (%wt)

No coating Elements	2% pectin	1% pectin & 1% alginate	1% pectin & 1% carrageenan	1% pectin & 1% xylan	1% pectin & 1% xanthan
O	84.6±0.51	72.1±0.76	74.9±0.53	81.8±0.07	83.2±0.88
Na		14.0±0.64			
S			8.8±0.19		
Zn	15.4±0.51	13.6±0.42	10.2±0.87	18.2±0.07	16.2±0.86

Table 4.2 Elemental analysis of the surface of coated films (%wt)

PSSMA coating Elements	2% pectin	1% pectin & 1% alginate	1% pectin & 1% carrageenan	1% pectin & 1% xylan	1% pectin & 1% xanthan
O	78.2±1.94	75.9±0.29	74.6±0.59	80.2±0.88	78.0±1.86
Na	2.2±0.36	6.8±0.23	5.0±0.16	2.1±0.54	4.2±1.55
S	2.8±0.16	2.7±0.16	7.7±0.15	1.9±0.08	2.9±0.10
Zn	16.8±0.12	14.6±0.47	8.6±0.69	15.8±0.85	14.5±1.51

Generally, Zn found in all films directly originated from the crosslinking agent – zinc acetate solution. There was no apparent change in the weight percentage of zinc before and after coating with PSSMA and thus, most zinc seems to be locked in the "egg-box" structure of pectin. Even though PSSMA might have competed with anionic groups in polysaccharides to bind with zinc at the film's surface, it is unlikely that zinc deprotonated in water. When comparing films without and with PSSMA coating, it can clearly be seen in the coated films that both sodium and sulfur were involved to the films' surfaces. This can be attributed to the presence of sulfonate and carboxyl groups in the sodium salt form of PSSMA (Fig. 4.2) and is evidence for the formation of a coating on all films, irrespective of their composition. Alginate was in its sodium salt form, which added some sodium to the film before coating was performed. The comparatively high sulfur content in carrageenan containing films is an indicator of its sulfate groups and remained present after coating to a certain extent which shows that the PSSMA coating did not completely exclude the surface of the original film.

4.3.4 Mechanical properties analysis

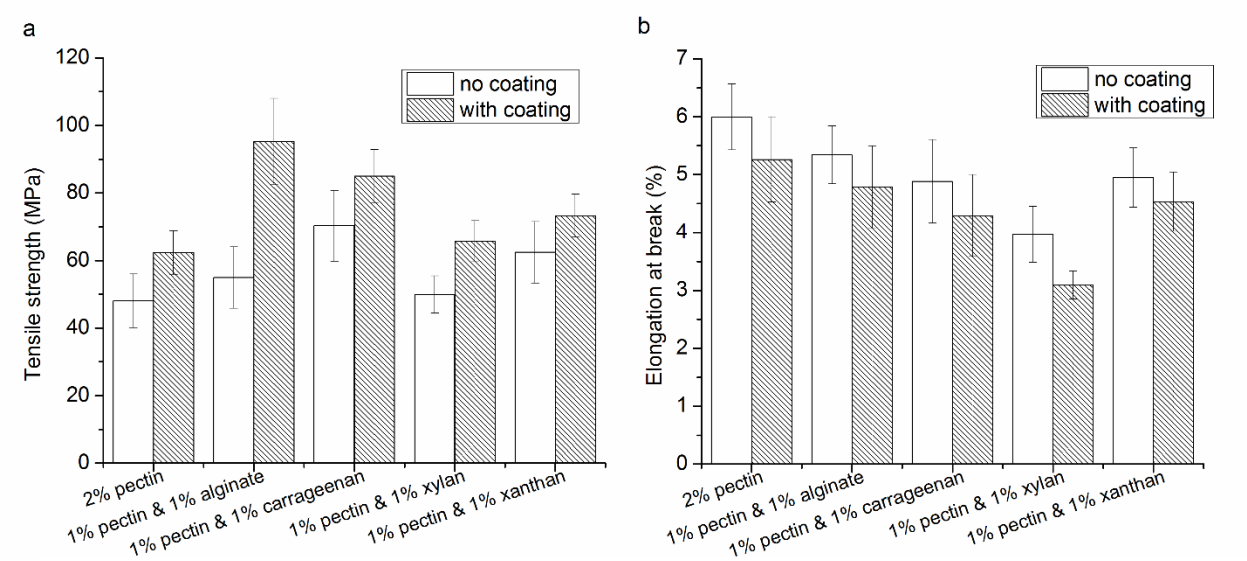

Fig. 4.6 Mechanical properties of films (a) without PSSMA coating, (b) with PSSMA coating

PSSMA coating was applied to the films with the purpose of enhancing their sorption capabilities for pollutants and as a side-effect, not the main goal, to improve their mechanical properties. Tensile strength (Fig. 4.6a) and elongation at break (Fig. 4.6b) of coated and uncoated films were investigated and compared. It was found that the tensile strength values were reasonably high while the values for elongation at break (%) were fairly low, indicating some brittleness as a consequence of decreased flexibility of the polysaccharide chains after crosslinking, even though glycerol had been added as plasticizer to all film compositions. PSSMA coating played a role in increasing the films' tensile strength by the formation of a dense and fairly strong outer layer on the polysaccharide films, but it did not significantly increase their elongation at break and flexibility. The mechanical properties of the films, however, were sufficient for their intended purpose and all experiments performed.

4.3.5 Methylene blue (MB), crystal violet (CV), cetylpyridinium chloride (CPC) and

benzethonium chloride (BtCl) sorption

It was assumed that films prepared with different anionic polysaccharides still contain a certain amount of available negatively charged groups (carboxyl and sulfate groups) after crosslinking in neutral solutions (pH 6-7). These extra negative charges could then form electrostatic interactions with the positively charged groups in both dyes, MB and CV as well as in both antiseptics, CPC and BtCl, and adsorb them from water. The chemical structures of these compounds are shown in Fig. 4.7. Besides available negative charges, the large surface area of the films was expected to expose a sizeable amount of sorption sites for the cationic compounds. It was expected that the incorporation of PSSMA coating on films' surfaces could further increase cation sorption. The obtained results are shown in Figs. 4.8 to 4.11.

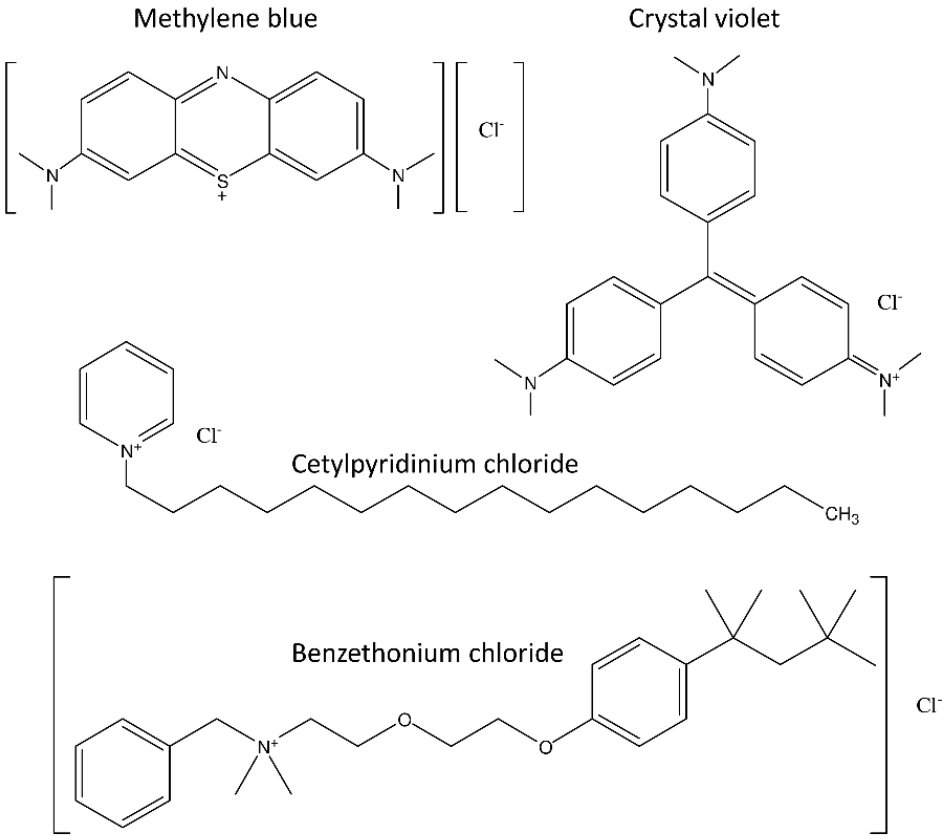

Fig. 4.7 Chemical structures of MB, CV, CPC and BtCl

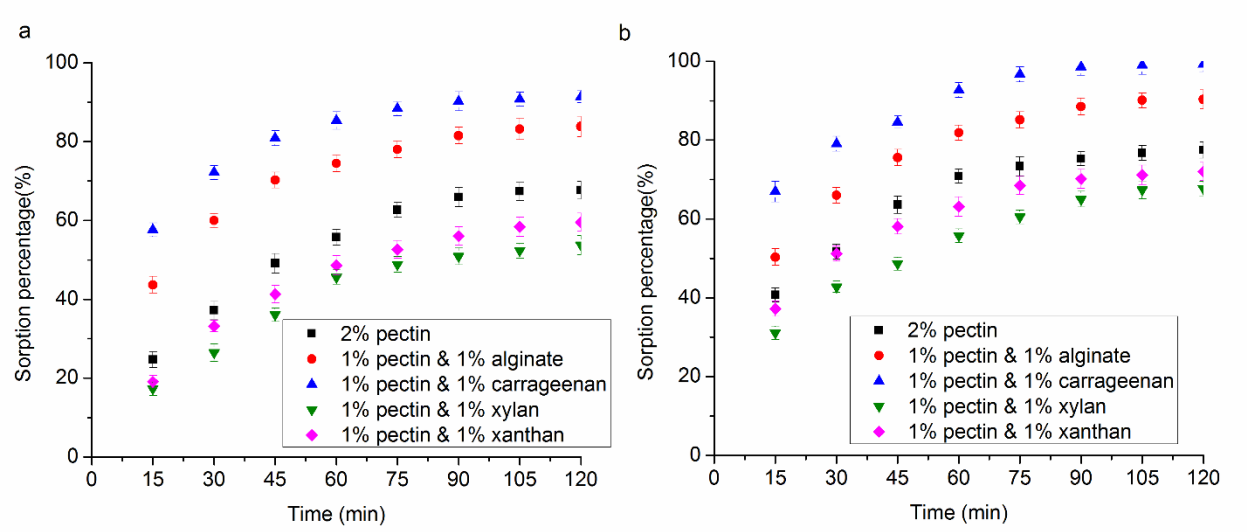

Fig. 4.8 MB sorption on (a) uncoated films, (b) PSSMA-coated films

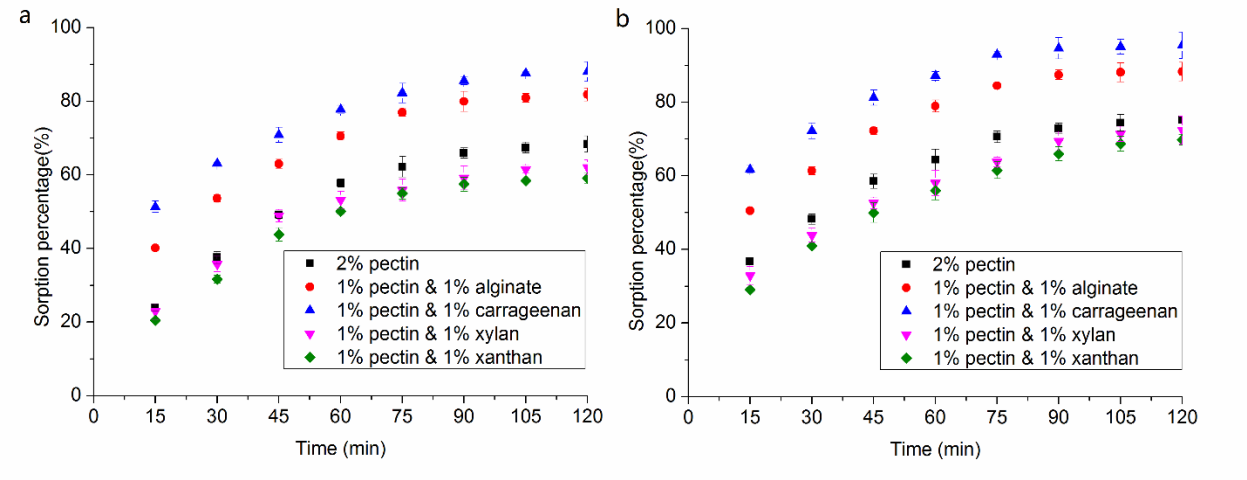

Fig. 4.9 CV sorption on (a) uncoated films, (b) PSSMA-coated films

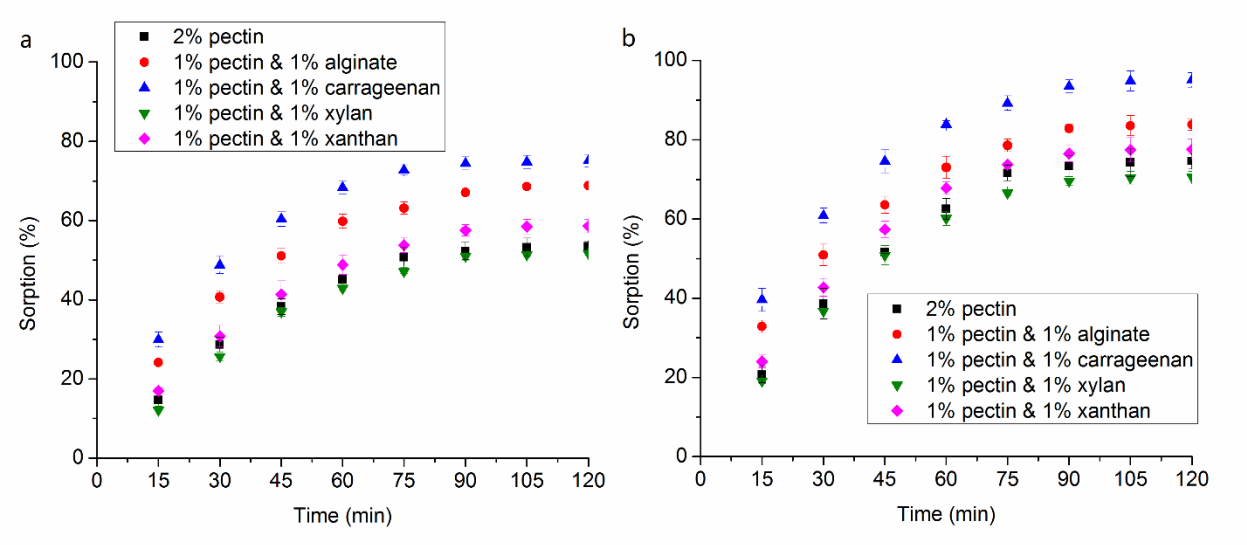

Fig. 4.10 CPC sorption on (a) uncoated films, (b) PSSMA-coated films

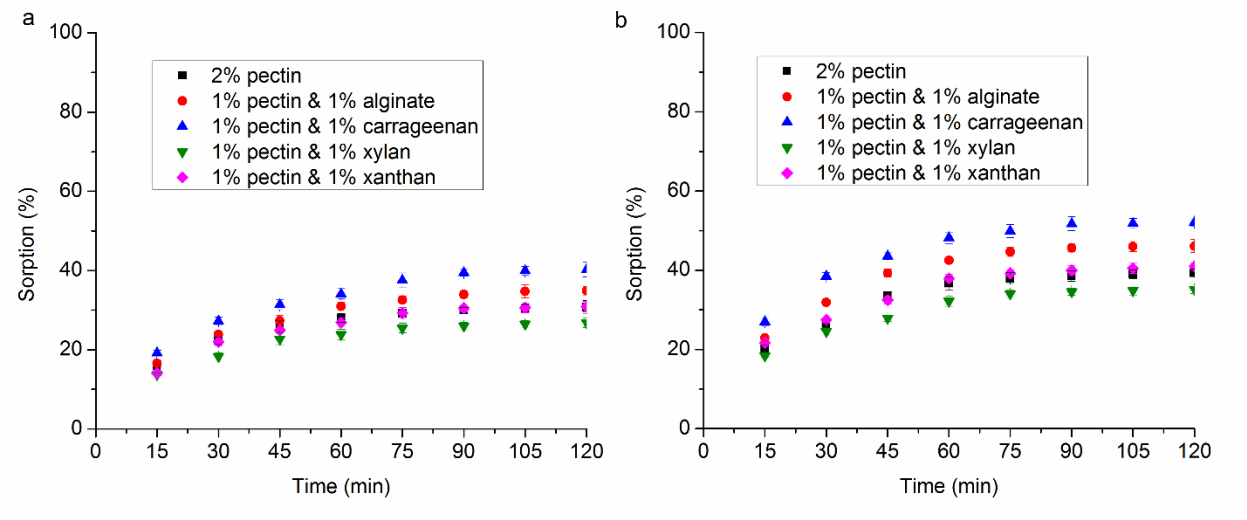

Fig. 4.11 BtCl sorption on (a) uncoated films, (b) PSSMA-coated films

Figs. 4.8 to 4.11 illustrate that both material composition and PSSMA coating lead to major differences in the sorption capabilities of the films for the investigated four cationic compounds. Without coating, films containing carrageenan and alginate showed the highest amount of sorption. Higher sorption of dyes and antiseptics indicates the presence of more and stronger electrostatic interaction in carrageenan and alginate. Alginate was able to considerably swell in water (see Fig.

4.3), especially after coating with PSSMA. Carrageenan contains a large amount of sulfate groups which can interact with cationic compounds. EDS had shown that these groups are available on the surface even after coating (see Table 4.2). The overall lowest sorption for all types of films was observed with xylan as admixture. It is possible that it had less anionic groups than an equal amount of any of the other anionic polysaccharides. In addition, xylan as filler in the film might reduce the accessible internal surface area as well as the amount of exposed anionic sites for positively charged groups.

The concentration of CPC and BtCl with 150 mg/L in water was higher than that of the dyes (5 mg/L) because both antiseptics could not be detected by UV-vis measurements at the dyes' low initial concentration. Therefore, the sorption capacity of the antiseptics at equilibrium seems larger than that of the dyes at first glance. From the results it can be assumed that besides the composition of the films, the type of cationic compound also affected the sorption on the films. Both dyes are small molecules with non-localized cationic charges (Fig. 4.7) which might have resulted in an easier contact with the negative charges in the film and which is reflected in increased sorption. Both dyes were almost completely removed by coated films composed of pectin and carrageenan.

It was further observed that films with PSSMA coating (Figs. 4.8b, 4.9b, 4.10b and 4.11b) had higher sorption by 8%-26% for MB/CV and 21%-39% for CPC/BtCl at equilibrium than films without coating (Figs. 4.8a, 4.9a, 4.10a and 4.11a), clearly due to the higher amount of available negatively charged groups on the film surfaces. As could be expected, in this series films containing carrageenan and alginate still showed the highest sorption capability, as cationic compounds could interact with larger amounts of negatively charged groups both in- and outside these films.

4.3.6 Sorption kinetics studies

The sorption capacities at equilibrium (q_e), rate constants (k_1 or k_2) and correlation coefficients (R^2) were calculated and are listed in Table 3 for uncoated films and Table 4 for coated films. The sorption processes occurred quite rapidly and most of the cationic compounds could be removed within the initial 90 min. Thus, both pseudo-first-order and pseudo-second-order were fitted and adjusted to the data from the first 90 min of the experiments.

For pseudo-first-order model, the plot of $\ln(q_e-q_t)$ against t resulted in a straight line with the slope of k_1 and intercept of $\ln q_e$. As can be seen from Tables 3 and 4, the correlation coefficient for the sorption of cationic model compounds on uncoated films ranged from 0.903 to 0.995 and on coated films from 0.925 to 0.998. Better agreement could be achieved applying the pseudo-second-order kinetic model.

Table 4.3 Kinetic parameters of MB, CV, CPC and BtCl sorption onto uncoated anionic polysaccharide films

Film composition (uncoated)		Pseudo-first-order			Pseudo-second-order		
		q_e (mg/g)	k_1 (min^{-1})	R^2	q_e (mg/g)	k_2 (g mg^{-1} min^{-1})	R^2
2% pectin	MB	0.780	0.042	0.955	0.770	0.026	0.995
	CV	0.702	0.038	0.977	0.783	0.025	0.996
	CPC	22.8	0.047	0.969	23.9	$4.90*10^{-4}$	0.954
	BtCl	6.46	0.040	0.995	8.23	0.006	0.999
1% pectin &	MB	0.536	0.036	0.983	0.736	0.073	0.999

1% alginate	CV	0.718	0.040	0.962	0.765	0.051	0.996
	CPC	22.0	0.041	0.969	23.3	$9.16*10^{-4}$	0.995
	BtCl	8.41	0.039	0.980	9.73	0.004	0.999
1% pectin & 1% carrageenan	MB	0.541	0.044	0.988	0.767	0.109	1.000
	CV	0.543	0.035	0.974	0.751	0.080	0.997
	CPC	31.3	0.056	0.971	24.0	0.001	0.994
	BtCl	11.2	0.042	0.932	11.2	0.003	0.997
1% pectin & 1% xylan	MB	0.544	0.035	0.986	0.681	0.022	0.970
	CV	0.506	0.034	0.988	0.651	0.038	0.988
	CPC	26.9	0.050	0.903	21.6	$5.99*10^{-4}$	0.971
	BtCl	5.52	0.038	0.992	7.25	0.007	0.998
1% pectin & 1% xanthan	MB	0.527	0.032	0.991	0.678	0.027	0.996
	CV	0.684	0.042	0.974	0.704	0.026	0.989
	CPC	24.9	0.046	0.935	24.5	$5.29*10^{-4}$	0.987
	BtCl	9.51	0.047	0.930	8.79	0.004	0.998

Table 4.4 Kinetic parameters of MB, CV, CPC and BtCl sorption onto coated anionic polysaccharide films

Film composition (uncoated)		Pseudo-first-order			Pseudo-second-order		
		q_e (mg/g)	k_1 (min-1)	R^2	q_e (mg/g)	k_2 (g mg^{-1} min^{-1})	R^2
2% pectin	MB	0.551	0.039	0.993	0.703	0.067	0.996

	CV	0.600	0.037	0.978	0.701	0.055	0.996
	CPC	37.4	0.051	0.950	34.7	$3.14*10^{-4}$	0.967
	BtCl	9.32	0.045	0.993	10.9	0.004	0.994
	MB	0.488	0.029	0.998	0.786	0.075	0.999
1% pectin &	CV	0.832	0.048	0.933	0.788	0.066	0.996
1% alginate	CPC	33.6	0.050	0.925	27.1	$9.18*10^{-4}$	0.999
	BtCl	14.1	0.051	0.982	13.0	0.003	0.998
	MB	0.705	0.050	0.949	0.829	0.105	0.998
1% pectin & 1%	CV	0.767	0.050	0.943	0.812	0.091	0.997
carrageenan	CPC	30.0	0.045	0.964	29.0	0.001	0.999
	BtCl	16.2	0.053	0.934	14.2	0.004	0.999
	MB	0.531	0.033	0.950	0.627	0.056	0.991
1% pectin & 1%	CV	0.573	0.032	0.935	0.673	0.050	0.990
xylan	CPC	35.1	0.051	0.949	33.1	$3.27*10^{-4}$	0.947
	BtCl	9.55	0.047	0.976	9.73	0.005	0.996
	MB	0.527	0.039	0.979	0.645	0.076	0.999
1% pectin & 1%	CV	0.544	0.030	0.972	0.670	0.044	0.995
xanthan	CPC	35.3	0.051	0.963	31.1	$4.82*10^{-4}$	0.979
	BtCl	9.64	0.042	0.981	11.3	0.004	0.993

The pseudo-second-order rate constant k_2 and the equilibrium sorption capacity q_e can be determined from the slope and intercept of the plot of t/qt versus t. From Tables 4.3 and 4.4, higher correlation coefficients of 0.951-1 for uncoated films and 0.947-0.999 for coated films were

obtained for sorption of all investigated cationic compounds by almost all films with different compositions. Therefore, pseudo-second-order kinetics seems to better fit the experiments. Pseudo-second-order is based on the assumption that the rate limiting step is the chemical sorption or chemisorption involving valency forces between sorbent and sorbate [33]. Thus, it appears to more suitably represent the sorption of both cationic dye and antiseptic model compounds by the investigated film compositions.

From the calculated rate constants k_2, the efficiency of a sorbent can be assessed. Larger values for k mean faster removal of a pollutant from water and higher efficiency as sorbent. The q_e value gives an indication of the amount of pollutant that is potentially removed at equilibrium. Thus, a higher q_e is also associated with the efficiency of the sorbent. The rate constant k_2 and the sorption capacity at equilibrium q_e calculated from experimental data of coated films were to the most part larger than those of uncoated films. Overall, k_2 and q_e of films containing carrageenan and alginate had generally higher sorption capacity for most of the four cationic compounds and thus seemed to be the most effective sorbents. The results obtained from the pseudo-second-order model matched well with the experimental data presented in the previous sorption section.

4.4 Conclusions

A series of anionic polysaccharide films were prepared from pectin with alginate, carrageenan, xylan or xanthan and crosslinked with zinc ions. It was found that different properties, including films thicknesses, swelling properties, surface morphologies, and mechanical properties were highly affected by the properties of the admixed polysaccharides and further enhanced by an additional PSSMA coating. The sorption capacity for cationic compounds was influenced mostly by polysaccharides' available anionic groups in the films after crosslinking as well as the nature

of the cationic compounds. As could be expected, alginate and carrageenan containing more negatively charged groups compared to the other polysaccharides investigated in this study had the highest cationic compound sorption percentage. Overall, films with PSSMA coating showed smoother film surface and enhanced tensile strength, In addition, for the removal of cationic contaminants from water, especially for dyes in trace amount, all films showed higher sorption than uncoated films. Among them, alginate and carrageenan were the most effective admixtures to pectin. PSSMA coating further enhanced the sorption capability of the films.

4.5 References

[1]. Stiborova H, Kolar M, Vrkoslavova J, Pulkrabova J, Hajslova J, Demnerova K, Uhlik O (2016) Linking toxicity profiles to pollutants in sludge and sediments, J Hazard Mater, http://dx.doi.org/doi:10.1016/j.jhazmat.2016.09.051

[2]. Chaukura N, Gwenzi W, Tavengwa N, Manyuchi MM (2016) Biosorbents for the removal of synthetic organics and emerging pollutants: Opportunities and challenges for developing countries, Environ Dev 19: 84-89

[3]. Sui Q, Cao X, Lu S, Zhao W, Qiu Z, Yu G (2015) Occurrence, sources and fate of pharmaceuticals and personal care products in the groundwater: A review, Emerging Contaminants 1: 14-24

[4]. Segura PA, Francois M, Gagnon C, Sauve S (2009) Review of the occurrence of anti-infectives in contaminated wastewaters and natural and drinking water, Environ Health Perspect 117: 675-684

[5]. Carvalho IT, Santos L (2016) Antibiotics in the aquatic envionments: A review of the European scenario, Environ Int 94: 736-757

[6]. Robinson T, Mcmullan G, Marchant R, Nigam P (2001) Remediation of dyes in textile effluent: a critical review on current treatment technologies with a proposed alternative, Bioresourse Technol 77: 247-255

[7]. Barakat MA (2011) New trends in removing heavy metals from industrial wastewater, Arabian J Chem 4: 361-377

[8]. Bansal RC, Goyal M (2005) Activated carbon adsorption, CRC press

[9]. Selvaraju G, Nor Kartini Abu Bakar (2017) Production of a new industrially viable green-activated carbon from Artocarpus integer fruit processing waste and evaluation of its chemical, morphological and adsorption properties, J Clean Prod 141: 989-999

[10]. Gupta VK, Suhas (2009) Application of low-cost adsorbents for dye removal--a review. J. Environ Manage 90: 2313-2342

[11]. Sriamomsak P (2003) Chemistry of pectin and its pharmaceutical uses: A review, Silpakorn University Int J 3: 206-228

[12]. Braccini I, Perez S (2001) Molecular basis of Ca^{2+}-induced gelation in alginates and pectins: The egg-box model revisited, Biomacromolecules 2: 1089-1096

[13]. Robitzer M, David L, Rochas C, Renzo FD, Quignard F (2008) Nanostructure of calcium alginate aerogels obtained from multistep solvent exchange route. Langmuir 24: 12547-12552

[14]. Liu S, Li L (2016) Thermoreversible gelation and scaling behavior of Ca^{2+}-induced κ-carrageenan hydrogels, Food Hydrocolloid, 61: 793-800

[15]. Xu L, Dong M, Gong H, Sun M, Li Y (2015) Effects of inorganic cations on the rheology of aqueous welan, xanthan, gellan solutions and their mixtures, Carbohyd Polym, 121, 147-154

[16]. Li M, Tshabalala MA, Buschle-Diller G (2016) Formulation and characterization of polysaccharide beads for controlled release of plant growth regulators, J Mater Sci 51: 4609-4617

[17]. Torres E, Mata YN, Blazquez ML, Munoz JA, Gonzalez F, Ballester A (2005) Gold and silver uptake and nanoprecipitation on calcium alginate beads, Langmuir 21: 7951-7958

[18]. Chen JP, Tendeyong F, Yiacoumi S (1997) Equilibrium and kinetic studies of copper ion uptake by calcium alginate, Environ. Sci. Technol. 31: 1433-1439

[19]. Gotoh T, Matsushima K, Kikuchi KI (2004) Preparation of alginate-chitosan hybrid gel beads and adsorption of divalent metal ions, Chemosphere 55: 135-140

[20]. Guibal E, Milot C, Tobin JM (1998) Metal-anion sorption by chitosan beads: equilibrium and kinetic studies, Ind Eng Chem Res 37: 1454-1463

[21]. Anca MY, Arpa C, Ergene A, Bayramoglu G, Genc O (2003) Ca-alginate as a support for Pb (II) and Zn (II) biosorption with immobilized Phanerochaete chrysosporium. Carbohyd Polym 52: 167-174

[22]. Bertagnolli C, Grishin A, Vincent T, Guibal E (2016) Recovering heavy metal ions from complex solutions using polyethylenimine derivatives encapsulated in alginate matrix, Ind Eng Chem Res 55: 2461-2470

[23]. Cataldo S, Cavallaro G, Gianguzza A, Lazzara G, Pettignano A, Piazzese D, Villaescusa I (2013) Kinetic and equilibrium study for cadmium and copper removal from aqueous solutions by sorption onto mixed alginate/pectin gel beads, J Environ Chem Eng 1: 1252-1260

[24]. Aravindhan R, Fathima NN, Rao JR, Nair BU (2007) Equilibrium and thermodynamic studies on the removal of basic black dye using calcium alginate beads, Colloid Surface A 299: 232-238

[25]. Li M, Elder T, Buschle-Diller G (2016) Alginate-based polysaccharide beads for cationic contaminant sorption from water, Polym Bull, DOI:10.1007/s00289-016-1776-2

[26]. Li M, Ziem S, Buschle-Diller G (2015) Morphology of polysaccharide beads and films for

environmental and biomedical applications, Earth day, UT Knoxville

[27]. Mahamadi C, Mawere E (2013) Kinetic modeling of methylene blue and crystal violet dyes adsorption on alginate-fixed water hyacinth in single and binary systems, AM J Anal Chem 4: 17-24

[28]. Djebri N, Boutahala M, Chelali NE, Boukhalfa N, Zeroual L (2016) Enhanced removal of cationic dye by calcium alginate/organobentonite beads: Modeling, kinetics, equilibriums, thermodynamics and reusability studies, Int J Biol Macromolec 92: 1277-1287

[29]. Inal M, Erduran N (2015) Removal of various anionic dyes using sodium alginate/poly(N-vinyl-2-pyrrolidone) blend hydrogel beads, Polym Bull 72: 1735-1752

[30]. Deng H, Xu Y, Zhu B, Wei X, Liu F, Cui Z (2008) Polyelectrolyte membranes prepared by dynamic self-assembly of poly (4-styrenesulfonic acid-co-maleic acid) sodium salt (PSSMA) for nanofiltration (I), J Membrane Sci, 323: 125-133

[31]. Song Y, Lv S, Cheng C, Ni G, Xie X, Huang W, Zhao Z (2015) Fast and highly-efficient removal of methylene blue from aqueous solution by poly(styrenesulfonic acid-co-maleic acid)-sodium-modified magnetic colloidal nanocrystal clusters, Appl Surf Sci, 324: 854-863

[32]. Qiu H, Lv L, Pan B, Zhang Q, Zhang W, Zhang Q (2009) Critical review in adsorption kinetic models, J Zhejiang Univ Sci A 10: 716-724

[33]. Elzatahry, AA., Soliman, EA., Mohy Eldin, MS, Elsayed Youssef, M. (2010) Experimental and simulation study on removal of methylene blue dye from alginate micro-beads, J Am Sci 6: 846-851

Chapter 5 Conclusions

Crosslinking alginate or pectin and forming beads or films in the presence of one other polysaccharide as admixture results in improved mechanical properties and less solubility in water of the product materials. The beads and films are capable of developing electrostatic interactions with oppositely charged functional groups and could be used to achieve the goal of removing cationic pollutants from water as well as acting as controlled release agents for agrochemicals with negatively charged groups.

The polysaccharide beads and films were further modified by adding kaolin as filler for enhanced mechanical properties and polyelectrolyte coating to control their sorption/release capacity for charged compounds. It was found that with a positively charged coating of PEI, the cumulative release of PAA could be slowed down significantly; with a negatively charged PSSMA surface coating on films, increased sorption of cationic dyes as exemplified by MB and CV, as well as antiseptic compounds, such as CPC and BtCl, could be realized.

In summary, polysaccharides are well-suited to be shaped into effective functional sorbents in form of beads and films and thus into materials for application in water decontamination and controlled delivery of active compounds. Polysaccharides originate from nontoxic renewable resources and both materials and processing methods are cost-effective. This research reflects some of the integral properties of these materials and demonstrates potential opportunities for wide-spread future applications.